AIMS Geosciences

AIMS Geosciences, 12(1): 001–051.
DOI: 10.3934/geosci.2026001
Received: 17 June 2025
Revised: 24 August 2025
Accepted: 17 October 2025
Published: 04 January 2026

https://www.aimspress.com/journal/geosciences

*Research article*

# Field to laboratory shear strength ratio for clays stabilized with low-carbon binders

**Juha Forsman[1,2,*], Monica Löfman[1,2], Jari Ikävalko[1] and Leena Korkiala-Tanttu[2]**

[1] Department of Geotechnical Engineering, Ramboll Finland Oy, Itsehallintokuja 3, Espoo, 02601, Finland
[2] Department of Civil Engineering, Aalto University, 02150, Espoo, Finland

* **Correspondence:** Email: juha.forsman@ramboll.fi; Tel: +358 40 583 3287, Fax: +358 20 755 6201.

**Abstract:** The carbon dioxide emissions of a low-carbon deep mixing binder can be up to 80–90% lower compared with, for example, lime–cement binder emissions. The transition to low-carbon binders is ongoing in deep mixing, and thus studying the curing and optimization of the binder content of clay stabilized with low-carbon binders is necessary to develop design processes. In Finland, since 2001, a field to laboratory strength ratio is used to determine the design strength of stabilized clay if quality control (QC) soundings of the earlier representative columns are not available. The objective of this study was to determine field to laboratory strength ratios for low-carbon binders based on laboratory stabilization tests and QC soundings. The data consist of six stabilization test sites implemented with 11 different low-carbon binders and lime–cements. The laboratory specimens were made with the same clay, binder recipe, and curing time as the test columns. The binders discussed in this study are divided into four groups on the basis of their raw material compositions: Calcareous, gypsum, blast furnace slag, and fly ash. The results showed that when the laboratory shear strength is low, the field-to-laboratory strength ratio is higher than when laboratory shear strength is high. Further, with gypsum-, blast furnace slag-, and fly ash-containing binders, higher shear strengths were often achieved in the laboratory than in the test columns. With calcareous binders, higher strengths were frequently achieved in the test columns than in the laboratory. The extensive data were used to derive trendlines (laboratory shear strength versus field to laboratory strength ratio) for the four binder types. Trendlines can be used to predict the characteristic shear strength value of stabilized clay from

laboratory strength. In addition, the uncertainty related to the prediction was quantified. These trendlines for low-carbon binders will be used in the revision of the Finnish guidelines.

**Keywords:** clay; deep mixing; low-carbon binder; field to laboratory strength ratio; QC sounding

## 1. Introduction

The Institute of Environmental Management and Assessment (IEMA) has presented a hierarchy for carbon reduction: Eliminate, reduce, substitute and compensate [1]. The European Federation of Foundation Contractors (EFFC) and The Deep Foundation Institute (DFI) have identified the top key ways to decarbonize certain parts of geotechnical construction via this hierarchy presented by IEMA: Eliminate (e.g., prevent GHG emissions across the life cycle), reduce (e.g., optimize designs and approaches), substitute (e.g., purchase materials with lower embodied carbon), and compensate (e.g., use technologies that are carbon-negative) [2]. In deep mixing, the abovementioned goals may mean, for example, the sustainable life cycle design, the optimization of the binder recipe (quality and content), and the use of low-carbon binders, the latter two of which are discussed in this article. Prevention of greenhouse gases (GHG) across the life cycle of deep mixed structures is presented elsewhere (e.g., [3,4]). A low-carbon waste material-based cement is also a solution that enables the reduction of the carbon footprint on an industrial scale by up to 90% compared with traditional cement production [5]. If captured carbon dioxide is bound to the deep mixed soil or if biochar is used as a component in the binder, it is possible to implement carbon-negative deep mixing (e.g., [6–8]). In the concrete industry, the utilization of captured carbon dioxide is more developed, and the manufacture of concrete elements utilizing captured carbon dioxide producing carbonated products is already on a commercial scale [9]. For the geotechnical engineering industry, the EEFC and the DFI have developed a carbon calculator which provides a full cradle-to-grave carbon assessment for a geotechnical solution. According to that calculation, the components of the carbon calculation for a typical soil mixing project show that the contribution of the materials (mainly binders) is 77% [4]. In dry Finnish deep mixing projects, up to over 90% of the emissions are related to the production and transport of lime–cement binders [10].

Deep mixing and other ground improvement methods are included in the new draft Eurocode proposal (prEN1997-3, Chapter 11). The design of deep mixing according to Eurocode 7 [11] is based on a concept of the characteristic strength value of the stabilized clay (soil mix), for which the design value is determined by dividing the characteristic value by partial factors. The proposal introduces a requirement to determine the strength of the stabilized soil (soil mix) from the characteristic strength value determined by laboratory or field tests. According to the guidelines of the Finnish Transport Infrastructure Agency (FTIA) [12], the characteristic shear strength value of stabilized soil ($\tau_{stab,k}$) is a cautious average value of the geotechnical parameters based on engineering judgement. The shear strength value of the soil mix ($\tau_{stab}$) is based on stabilization tests in the laboratory, quality control (QC) soundings of test columns, or QC soundings of previous stabilization sites in similar geotechnical conditions. In Finland, deep mixed columns are commonly used to increase stability and to control the settlement of road, street, or railroad embankments founded on soft subsoil such as clay.

The strength of the soil mix is affected by various factors such as the soil's properties (e.g., water content, pH, organic content), the type and content of the binder, the mixing degree, and the curing conditions. The effects of these factors are quite complex, making it challenging to directly determine field strength only through laboratory mix tests. Further, the strength of a soil mix cannot be predicted from the in situ characteristics of the soil [13]. When the characteristic shear strength of the soil mix ($\tau_{stab,k}$) is based on the mean shear strength obtained from stabilization tests, in Finnish practice, it is reduced using the field to laboratory strength ratio ($k_{F/L}$) (i.e., a correction factor) to consider the difference between field and laboratory conditions. Graphs showing the values of the field to laboratory strength ratios have been presented in the literature (e.g., Figure 1). In Japan, the strength ratios determined from cores from (mainly) dry mixed columns (DDM) and laboratory samples of cement range from 0.5 to 2, with most values being from 0.5 to 1.0 [13]. In other words, field strength tends to be lower. Indeed, the EuroSoilStab [14] guideline proposes that the field to laboratory strength ratio should be 0.2–0.5. The Federal Highway Administration's (FHWA) design manual *Deep Mixing for Embankment and Foundation Support* indicates that the field to laboratory strength ratio should be at least 0.5 [15].

For soft Bangkok clay, for a given water to cement ratio and for all curing times, the field to laboratory shear strength ratio is reported to be 0.7–1.0 for DDM columns when the assessed field strength is based on cores [16]. Madhyannapu et al. [17] found the field to laboratory strength ratio of 0.67–0.86 for wet mixed columns field cores to be of the same magnitude as DDM columns through a the comparison (binder lime–cement: 25–75%). Timoney [18] studied stabilized cement (CEMI) mini columns in the laboratory and carried out stabilization tests, for both of which, the soil mix was mixed with a large pan mixer and both were built by layered compaction. Columns were tested by pull-out resistance tests (PORTs) or push-in resistance tests (PIRTs). In Sweden, a PORT is referred to as a FOPS (förinstallerad omvänd pelarsondering, pre-installed reverse column penetrometer). In this article, a PIRT is referred to as a column penetrometer (CP) test. Column strengths in PORTs and CP tests were found to predominantly vary between 0.8 and 1.2 times that of the respective stabilization test shear strengths (PORT: 0.7–1.3; CP: 0.8–1.2). The variations in the ratios are due to different curing temperatures and densities, and the effects of trimming the column samples [18]. Andersson and Vesterberg [19] presented field and laboratory results of lime–cement mixing results with curing times of 7, 28, 50, and 91 days. The increase in strength in the field is significantly greater than in the laboratory over 7 d of curing time. In 28 to 91 d, the field to laboratory shear strength ratio seems to decrease compared with that for 7 days of curing, which is probably caused by the greater heat generation in the field in the early stages of curing. Field to laboratory strength is mainly about 0.6–2 for curing times 28 to 90 d (estimated from the figures of the report [19]). Paniagua et al. [20] reported higher field to laboratory shear strength ratios due to the combined effect of higher curing temperatures and stresses acting on the lime–cement column during curing.

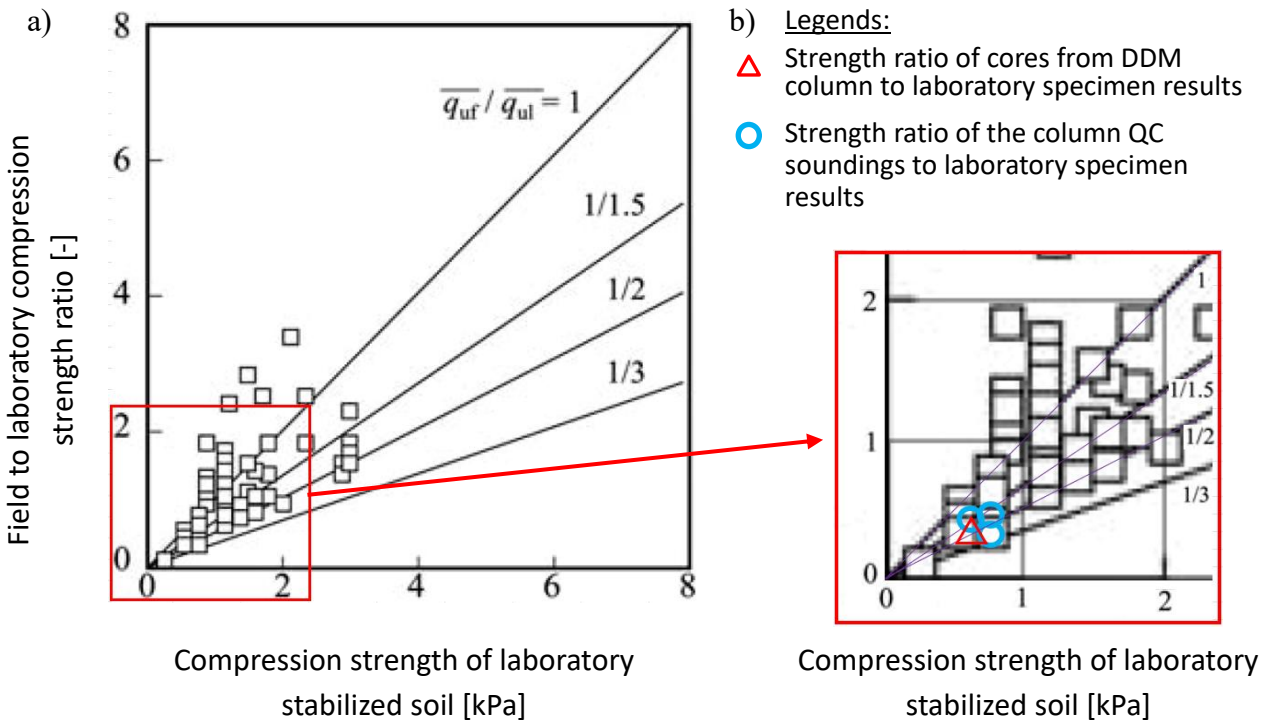


**Figure 1.** (a) The field to laboratory compression strength ratio for cores from DDM columns and laboratory samples (modified from [13]). (b) Ratios presented by Savila et al. [21] added to the figure.

Aalto [22] and Larsson [23] have compiled an extensive collection of field to laboratory shear strength ratios from the 1980s and 1990s from, e.g., Sweden, Finland, Norway, and Japan. The results presented by the Nordic researchers are mainly from lime cement column sites; Therefore, the graph compiled by Aalto (Figure 2b) represents deep lime cement column mixing and corresponds reasonably well with the FTIA's graph representing mixing with lime cement (Figure 2a). It should be noted that there are different views regarding the value of laboratory tests: Some researchers think that laboratory tests can only be used to optimize binder contents, some assume that there is a correlation between the strength obtained in a laboratory and the strength obtained in the field, and some assume that there is no correlation at all [24]. In the FTIA's guidelines, estimation of the design strength and the binder recipe from stabilization test results is performed, based on the first two assumptions. The procedure for the estimation of design strength for deep mixed columns from laboratory test results was first presented in the *Deep Stabilisation Design Guide* published in 1997 [25]. The field to laboratory strength ratio ($k_{F/L}$) nomogram was subsequently presented in the next design guide of the Finnish National Road Administration (FinRA) in 2001 [26], and the same nomogram is still in use (Figure 2a). The nomogram was originally presented without literature references, but in the 1990s, there were several deep stabilization studies undertaken at the Technical Research Centre of Finland (VTT) and Helsinki University of Technology (HUT), among others, and the consensus is that the nomogram was based on those results, adjusted by FinRA. In the nomogram, the $k_{F/L}$ ratio ranges from 0.6 to 1.0 for lime cement and from 0.4 to 0.7 for cement. The monogram does not present the low-carbon binders currently in use and under development, nor cement grades CEM III/A or CEM III/B. When the determination of the characteristic shear strength value of stabilized soil ($\tau_{stab,k}$) is

based on the stabilization test results, the nomogram of the FTIA (Figure 2a) is used as follows: If the $\tau_{stab}$ from stabilization tests is 150 kPa (e.g., 91 d of curing), the $k_{F/L}$ ratio can be read to be 0.93 for lime cement from the field to laboratory ratio axis. By using this $k_{F/L}$ ratio, the $\tau_{stab,k}$ is 140 kPa for a curing time of 91 d.

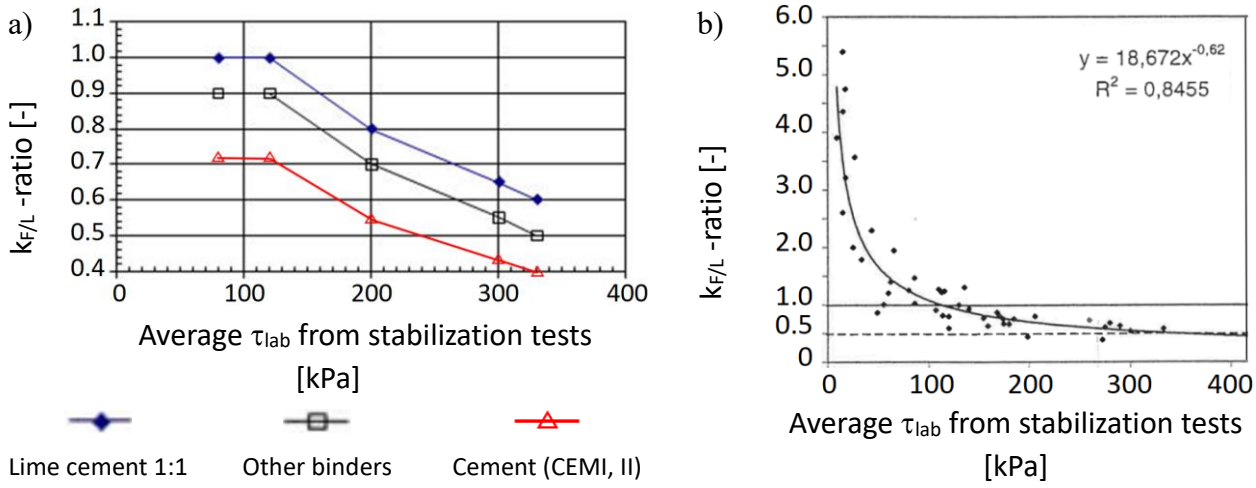


**Figure 2.** (a) The maximum value of the laboratory to field shear strength ratio $k_{F/L}$ for DDM in the *Deep Stabilisation Design Guide* of the FTIA (modified from [12]). (b) The $k_{F/L}$ ratio results from Sweden and Finland from the 1980s and 1990s for (predominantly) lime cement stabilized soil mixes (modified from [22]).

Larsson [27] stated that empirical relationships can only be found if the processing parameters of the laboratory tests are within the range of application of the method. This should be considered, and the minimum requirement would be that the factors which can be influenced by humans on the value of the $k_{F/L}$ ratio should be standardized: (1) All laboratories should carry out stabilization tests using the same procedure, (2) the determination of the design strength is specified in a guideline, (3) deep mixing is carried out in accordance with the same general work specification, and (4) QC soundings are carried out using the same procedure. In Finland, all four of these points have been realized since 2018: Points (1) and (2) are presented in the FTIA guideline [12], Point (3) in the general code of practice for construction of infrastructure [28] and Point (4) in both above. Before 2018, there was no national guideline for conducting stabilization tests, and laboratories conducted the tests using slightly different procedures. This problem has been observed elsewhere as well, e.g., [24].

Despite the shortcomings of the Finnish nomogram, it has been used for more than two decades, and it is likely that the absence of low-carbon binders in the nomogram and the lack of guidance have led to unnecessarily large binder dosages, ignoring low-carbon binders and thus causing additional binder costs and $CO_2$ emissions. Considering the above, the general consensus in the Finnish deep stabilization industry is that the nomogram is outdated and should be revised to include low-carbon binders that have been or are in the process of being used in deep mixing in production. The redefined $k_{F/L}$ nomogram will be based on test columns and stabilization tests carried out since 2018.

The reason for using alternative binders is not only to decrease cost but to decrease environmental impact [24]. The emission factor of a traditionally used lime cement binders is up to 5–10 times higher

than that of a low-carbon recycled binder [29,30]. The significance of binders for the carbon dioxide emissions of the site that is preconstructed with deep mixing can be illustrated by the preconstruction of the Malminkenttä area (Helsinki). According to the emission calculation, over 96% of the total emissions were caused by deep mixing with lime cement. With low-carbon binders, the emissions related to deep mixing can typically be reduced by 60–70%, which means a reduction in carbon dioxide equivalents of 200–240 million kg $CO_2e$ in the preconstruction of Malminkenttä [30].

Some low-carbon binders have been studied since the 1980s, such as gypsum [31,32]; fly ash (FA); blast furnace slag (BFS) [18,33–35]; FA (goal), desulfurated waste, and BFS [36]; gypsum, FA, and BFS [37–39]; and gypsum and slag [40]. In Finland, lime cement has been the state-of-the-art binder since the early 1980s. The low-carbon binder GTC (GTC = gypsum, calcium hydroxide and cement 1:1:1, FTC until 2008) has been used since the 1990s, but for most of the low-carbon binders, there is no such long-term experience.

The aim of this paper is to present the field to laboratory strength ratios $(k_{F/L})$_ of soil mixes stabilized with calcareous, gypsum-, BFS-, and FA-containing binders and to analyze the results via statistical methods. The laboratory shear strength was determined by uniaxial compression tests and these results were compared with the QC sounding results of the in situ soil mixes. The laboratory test results used in the determination of the $k_{F/L}$ ratio and their statistical data, such as the coefficient of variation (COV) are presented in this article. COV is a unitless measure of data dispersion, which can be used to quantify variability and uncertainty [41]. COV in the field strength results used to determine the ratio $k_{F/L}$ has been discussed elsewhere [42]. It is noteworthy that field strength can also be determined from samples taken from cured stabilized columns [21] or from test specimens made from uncured soil mixes in the field [13]. Likewise, the determination of the $k_{F/L}$ ratio is affected by uncertainty, and hence this article investigates the extent of data scatter around the newly derived nomogram's trendlines.

## 2. Materials and methods

### *2.1. Determination of the laboratory to field shear strength ratio $k_{F/L}$*

The field to laboratory shear strength ratio $k_{F/L}$ is determined by dividing the average shear strength of parallel QC soundings by the average shear strength from parallel uniaxial compression (UCS) test results (Equation 1, where laboratory shear strength is the compression strength divided by two, $\tau_{lab} = \sigma_{UCS}/2$).

$$k_{F/L} = \tau_{field} / \tau_{lab} \quad (1)$$

Test columns and stabilization test samples are stabilized with the same binder recipe using the same clay and curing time. The comparison with the QC sounding result ($\tau_{field}$) is made at the depth from which the clay samples were taken. When the result pairs ($k_{F/L}$ and laboratory shear strength $\tau_{lab}$) are available from several sites and soil layers where the strengths of the soil mixes vary over a sufficiently wide strength range, it is possible to create nomograms from the resulting pairs.

The principle of determination of the resulting pairs of field shear strength + laboratory shear strength is shown in Figure 3. In total, 83 similar figures have been processed, but the other 82 analogous figures are not presented in this article. Each figure has one to three pairs of results,

depending on how many depths clay samples have been taken from for the stabilization tests. In practice, clay samples have been taken for the stabilization tests from depths ranging almost up to 1 m, so a reference value for field shear strength $\tau_{field}$ has been determined for a depth interval of 1 m, corresponding to the sampling depth. Figure 3 presents a depth profile (0–9 m depth) with the line representing the mean shear strength according to QC soundings (in general, a mean of three to five parallel soundings). The short dashed vertical lines at depths of 2–3 m and 5.5–6.5 m represent the sampling depth of the clay used in the stabilization tests and the shear strength determined in the stabilization tests ($\tau_{lab}$). As shown in Figure 3, the shear strength based on QC soundings varies considerably between 5.5 and 6.5 m, so the chosen shear strength value $\tau_{field}$ represents the averaged values. On the other hand, the shear strengths determined by QC soundings can stay almost constant. Results where the strength varies are common, so instead of individual result pairs, it is more appropriate to examine the results derived from the nomograms formed from pairs of results (see Section 3.3).

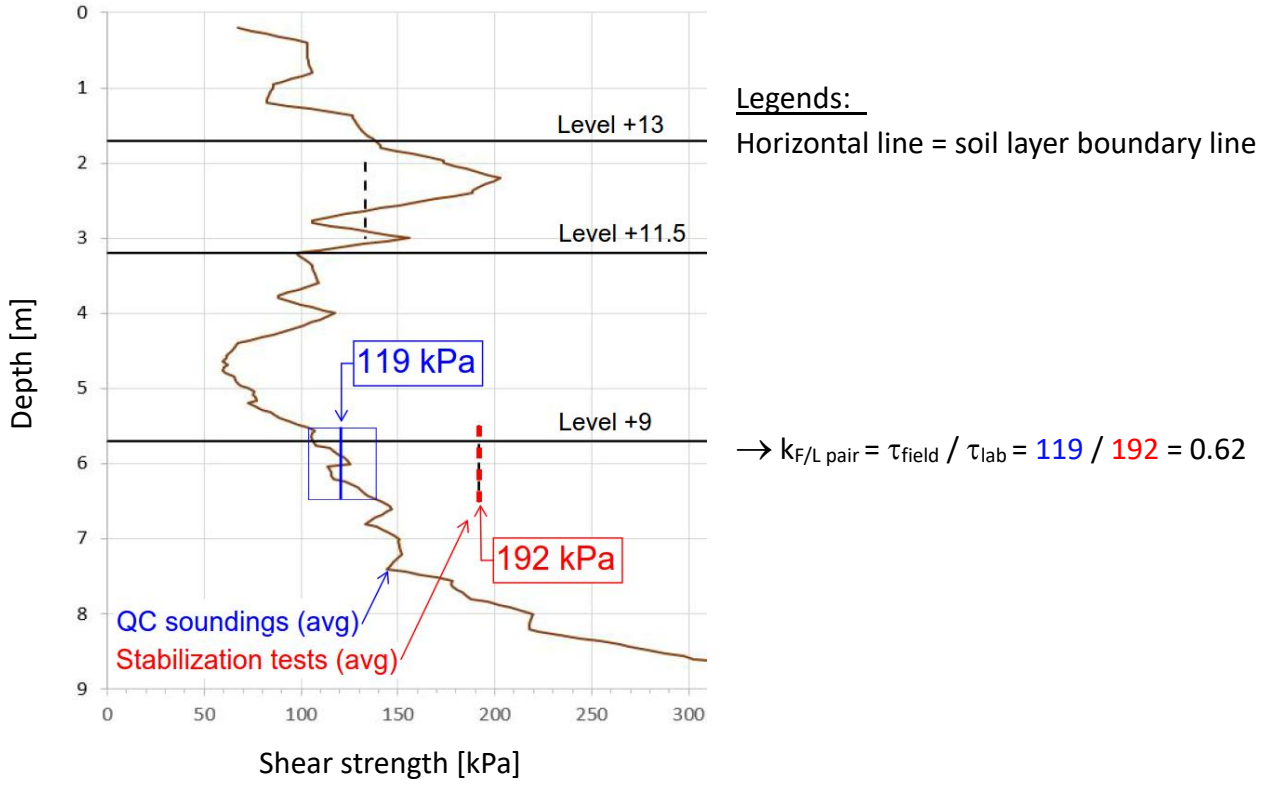


**Figure 3.** The average shear strength of parallel QC soundings and UCS tests, and the determination of $k_{F/L}$ pairs. Curing time, 91 d; test site T1 (S6), and GREEN binder.

*2.2. Test sites and soil properties*

The data in this study are from six different column stabilization test sites: Malminkenttä (Helsinki, T1), Luhtitie (Vantaa, T2), Kuninkaantammi (Helsinki, T3), Topinpuisto (Turku, T4), Länsiranta (Porvoo, T5), and Ilokkaanrinne (Tampere, T6). The city and object ID for each site are shown in parentheses. The locations and other information of the sites are presented in detail by Forsman et al. [42]. Sites T1, T2, and T4 are located in Southern Finland near Helsinki; Site T3 is

about 160 km west of Helsinki; and Site T6 is about 170 km north of Helsinki. At all sites, column stabilization is designed to be used as soil improvement for streets or yards to reduce settlement and to increase stability. All the studied columns are single columns, and the test sites do not include column lamellae where the columns intersect each other. The number of test fields is 91, with different binder recipes used at the six test sites. The index properties of the clay samples and the corresponding in situ vane shear strength for the test sites are presented in Table 1. All the stabilized soil layers examined in this study are clay, organic clay, or silty clay, with clay having at least 30% of grains with a particle size of 0–0.002 mm, and where the largest grains are in the fine silt grain range of 0.002–0.02 mm. The water permeability of Finnish clay is typically $10^{-9}$–$10^{-11}$ m/s.

The clay mineral composition of Finnish clays is predominantly illite and chlorite. Besides these, small proportions of vermiculite and kaolinite have been observed [32,43,44]. The soils prevailing in Finland were, for the most part, formed during the late glacial period 10,000–12,000 years ago. Very soft and watery fine-grained clays are primarily found in the coastal regions. The average clay thickness is about 10 m but can increase up to 60 m. Clays can be organic (i.e., organic content more than 2%) and they can be divided into geological sediment groups on the basis of the evolutionary stage of the Baltic Sea: Baltic Ice Lake, Yoldia Sea, Ancylus Lake, and Littorina Sea [45].

At some of the test sites, column-stabilized subsoil contains acid sulfate soil and sulfide-bearing soil (potential acid sulfate soil). Most of sulfide clays and organic clays have been identified in the coastal areas of the Baltic Sea, specifically in areas confined by the Littorina Sea. The Littorina Sea appeared in areas where the land level today is ≤35 m above sea level [46]. In test areas T3 and T6, the ground level is ≥30 and ≥105 m above sea level, respectively, so the presence of sulfide clay is unlikely. Sulfide clay is present in test areas T1, T2, T4, and T5. In test area T1, sulfide clay is active in the dry crust layer, and at a depth of about 1–3.5 m, it is potential [47]. None of the result pairs ($k_{F/L}$ and laboratory shear strength $\tau_{lab}$, see Section 2.1) are from dry crust layers with active sulfide clay. When sampling and performing stabilization tests on potential sulfide clay, special care has been taken to ensure that the clay samples are not oxidized before the stabilization test is performed.

**Table 1.** Index properties of the clay or organic clay at test stabilization sites T1–T6. "S1" means subarea [42].

| Site | Level (m above sea level) | Soil[a] | w[b] (%) | LOI[c] (%) | pH[d] (–) | $s_{tot}$[e] (g/kg) | $\tau_v$[f] (kPa) |
|---|---|---|---|---|---|---|---|
| T1, S1 | +15 to +14.2 | Dry crust | 120 | – | 3.9–5.9 | 6.0–13.6 | – |
| | +14.2 to +11 | Organic clay | 110–120 | 4.2–4.6 | 6.1–8.2 | 1.0–1.4 | 12–40 |
| | +11 to +8.5 | Clay | 85–135 | 3.8–4.7 | 6.1–6.9 | 1.8 | 8–9 |
| | +8.5 to +7.5 | Clay | 50–70 | – | – | – | 9–16 |
| T1, S4 | +15 to +13.5 | Dry crust | 85–150 | 3.8–5.1 | 5.7–7.3 | 1.0–10.0 | 12≤ |
| | +13.5 to +10.5 | Organic clay | 75–140 | 3.8–5.1 | 5.7–7.3 | 0.9–3.4 | 7–8 |
| | +10.5 to +9 | Clay | 105–120 | 4.2–4.9 | 5.4–6.9 | 2.1–2.6 | 7–9 |
| | +9 to +7.5 | Clay | 60–105 | 3.5–3.7 | 6.2–8.1 | 0.4 | 7–10 |

*Continued on next page*

| Site | Level (m above sea level) | Soil[a] | w[b] (%) | LOI[c] (%) | pH[d] (–) | $s_{tot}$[e] (g/kg) | $\tau_v$[f] (kPa) |
|---|---|---|---|---|---|---|---|
| T1, S6 | +15 to +13.5 | Dry crust | 80 | – | 4.2–6.5 | 0.15 | 30 |
| | +13.5 to +10.5 | Clay | 70–125 [g] | 3.8–6.4 | 5.7–7.0 | 0.6–18.3 | 7–9 |
| | +10.5 to +7.5 | Clay | 70–100 | 2.9–3.1 | 7.4–8.8 | 0.3 | 8–10 |
| | +7.5 to +6.0 | Clay | 25–80 | 2.9–3.1 | 7.4–8.8 | 0.3 | 10–12 |
| T2 | +29 to +28.5 | Dry crust | – | – | – | – | ≈50 |
| | +28 to +24 | Clay | 35–75 | 1.5–3.4 | 6.6–7.7 | – | 5–25 |
| T3 | +30 to +28 | Dry crust | ≈50 | – | – | – | 50–100 |
| | +28 to +26 | Clay | 50–60 | 3.5–4.9 | 7.1–8.2 | 0.3 | 20–40 |
| | +26 to +23 | Clay | 40–70 | 3.1–4.2 | 6.8–7.6 | - | 10–20 |
| T4 | +16 to +15 | Dry crust | 75 | – | – | – | – |
| | +15 to +10 | Clay | 60–130 | 0.7–4.5 | 6.5–7.5 | 0.5–1.4 | 12 [g] |
| | +10 to +6 | Clay | 80–120 | 0.5–3.8 | 6.5 | 0.3–1.4 | 12 [c] |
| T5, S1 | +0.8 to ±0 | Dry crust | – | – | – | – | |
| | ±0 to −3.0 | Organic clay | 130–175 | 7.0–8.2 | 7.8–8.1 | 18.0–19.4 | 8–10 |
| | −3.0 to −8 | Clay | 130–145 | – | – | – | 10–17 |
| | −8 to −16 | Clay | 80–110 | – | – | – | 5–10 |
| | −16 to −19 | Clay | 75–90 | – | – | – | ≈10–30 |
| T5, S2 | +1.3 to ±0 | Dry crust | 110 | – | – | – | – |
| | ±0 to −5.5 | Organic clay | 110–160 | 8.4 | 8.1 | 22.0 | 12–20 |
| | −5.5 to −11 | Clay | 80–120 | 4.0 | 7.7 | 1.6 | 12–23 |
| T5, S3 | +1.3 to +0.5 | Dry crust | 120 | – | – | – | – |
| | +0.5 to −5 | Organic clay | 125–150 | 7.4 | 8.0 | 20.0 | 7–12 |
| | −5 to −8.5 | Clay | 80–120 | – | – | – | 12–17 |
| | −8.5 to −16 | Clay | 95 | – | – | – | 8–10 |
| T6 | +105 to +101 | Dry crust | – | – | – | – | – |
| | +101 to +96 | Clay | 40 | 2.9 | 7.8 | – | 12–46 |

Notes: [a] [48]; [b] water content [49]; [c] loss on ignition, 550 ºC [50]; [d] pH value [51]; [e] total sulfur content [52]; [f] vane shear strength [53]; [g] there are also some thin silt layers where the water content is 25–70%.

### *2.3. Binders and binder content*

The binders in this study are low-carbon binders and lime cements. The raw materials and their proportions, pH, and grain size and the $CO_2$ emissions of the binders used are presented in Table 2. The emission per binder-ton ($CO_2$e/t) contains the production phases A1–A3 [54]. The $CO_2$ emission of the lime cement binder KC30 is over four times greater than the emissions of the binder mixture FA+CEM II. The emission factors of the binders KC20, KC30, GREEN, POZ, GTC, CEM III/A, and CEM III/B are based on environmental product declarations (EPDs). For the other binders, the unofficial emission factors are provided by the producers.

The binders discussed in this study are divided into four groups according to their raw material compositions: (1) Calcareous (GREEN, POZ, KC20, KC30), (2) gypsum-containing (GTC2, GTC3), (3)

BFS-containing (CEM III/A, CEM IIIB), and (4) FA-containing (JAM+CEM II, KAI+CEM II, KAU+CEM II, InfraStabi65, InfraStabi80). The reactions generated when mixing various binders with soil vary by process, intensity, and duration [55]. None of the binders consists of a single raw material, but they are all different mixtures and, for example, the binders GTC2 or CTC3 contains more lime compared with KC20 or KC30. However, they contain gypsum, which those classified as "calcareous" do not contain. In Finland, deep mixing binders are intended to be mixed by the dry stabilization method, so the binders must be dry. All binder raw materials presented in Table 2 are calcinated, incinerated, or dried. The raw materials are produced by calcination (CaO, $Ca(OH)_2$) or incineration (cement), or they are by-product or waste material from calcination, incineration, or energy production (lime kiln dust (LKD), BFS, FA). The gypsum of the binder GTC has been quarried in Spain and dried at the Nordkalk factory in Finland.

The expansion due to the newly formed ettringites in gypsum reactions is expected to significantly reduce the voids and thereby densify the stabilized clay, which plays a primary role in the strength gain [31,32]. FA in binders JAM+CEM II, KAI+CEM II, and KAU+CEM II are 100% bio-incineration ash: the JAM (Jämsänkoski paper mill) and KAI (Kaipola paper mill) FAs are formed via boiler combustion, and in the Jämsänkoski paper mill, the main fuels are paper mill bark (15–16%), fiber sludge (15–17%), wood chips (30–31%), sawmill by-products (20–27%), and peat (13–17%). Heavy fuel oil (0–0.5%) is used as the boiler's starting and supporting fuel. [56,57]. The proportion of the main components of JAM FA is 15–20%calcium (Ca), 7–12% silicon (Si), and 5–10% aluminum (Al) [58]. The fuel of the Kaukaa power plant (KAU) is wood-based and peat material, and the share of wood was 100% in December 2019 and 80% in April 2020. The wood-based fuel consists of bark, forestry industry side streams, forest crown mass, and mixed sludge from the biorefinery [58]. The proportion of the main components of KAU FA is 21–25% Ca, 7–10% Si, and 4–6% Al [59]. The main components of JAM FA determined by XRF (x-ray fluorescence spectroscopy) are 47.3% CaO. 21.7% $SiO_2$, and 13.3% $Al_2O_3$. JAM, KAI, and KAU FAs were not treated after removal from the silo of the mill or power plant before mixing with cement [47,57]. The binders InfraStabi65 and InfraStabi80 contain FA from burning biofuel and/or coal, and they can contain also LKD or FGD. (lime kiln dust or flue gas desulphurization gypsum). The ashes in the InfraStabi binders have been activated by pin mill treatment [56]. The content of calcium oxide in the InfraStabi binders is at least 13% [60].

The low-carbon binders and binder dosages per test sites are presented in Table 3. The binder contents have been selected according to the following criteria: The contents are typical of those used for column stabilization in Finland (70–200 kg/m$^3$); stabilization tests have been carried out to help in the selection of the content before stabilization with all binders; it is possible to achieve the target shear strength with at least one of the selected contents; and the contents of different binders are the same in parallel areas at one test stabilization site.

At Sites T1 and T4, all Finnish binder manufacturers were given the opportunity to deliver their binder to the stabilization contractor, as ordered by the developer, to be used in the test columns in accordance with the developer's test stabilization plan [61,62]. At Sites T2 and T6, the test stabilization was carried out as part of an extensive stabilization contract. The test stabilization at Site T5 was carried out by the developer and two binder manufacturers before the request for bids for an extensive stabilization contract. At Sites T2, T5, and T6, the developer approved the use of only three different

binders. At Site T3, the test stabilization was carried out in connection with the UUMA3 research project going on at that time, and the binder manufacturers were financiers of the research project [57].

**Table 2.** Raw materials and $CO_2$ emissions of the binders used in the stabilization tests and test columns to determine $k_{F/L}$ ratio (modified from [42]).

| Binder | The components of the binder and their proportions | | | | | Emissions |
|---|---|---|---|---|---|---|
| | Cement | Lime | Gypsum | BFS | FA | (kg $CO_2$e/t) |
| Calcareous binders (# 0–0.2 mm [b], pH 13.0–13.1 [b]) | | | | | | |
| KC20 [a] | 80% | CaO, 20% | – | – | – | 646 [a] |
| KC30 [a] | 70% | CaO, 30% | – | – | – | 758/741 [a] |
| GREEN [a] | 50% | LKD, 50% | – | – | – | 310/232 [a] |
| POZ [a] | 33% | CaO + LKD, 66% | – | – | – | 612/615 [a] |
| Gypsum-containing binders (# 0–1.6 mm [b], pH 12.9 [b]) | | | | | | |
| GTC2 [a] | 33% | $Ca(OH)_2$, 33% | 33% | – | – | 235 |
| GTC3 [a] | 33% | $Ca(OH)_2$, 33% | 33% | – | – | 209 |
| BFS binders (# 0–0.03 mm, pH 12.6) | | | | | | |
| CEM III/A | 100% | – | – | 36–65% | – | 446 |
| CEM III/B | 100% | – | – | 65–80% | – | 315 |
| FA-containing binders (# 0–0.1 mm [c] and 0–0.05 mm [d], pH 12.9–13.0) | | | | | | |
| JAM+CEM II | 30% | – | – | – | 70% | 184 |
| KAI+CEM II | 30% | – | – | – | 70% | 184 |
| KAU+CEM II | 30% | – | – | – | 70% | 184 |
| InfraStabi65 | 35% | – | – | – | 65% | – |
| InfraStabi80 | 20% | – | – | – | 80% | 144 |

$Ca(OH)_2$, calcium hydroxide; CaO, calcium oxide; LKD, lime kiln dust; BFS, blast furnace slag; KAI, Kaipola paper mill; JAM, Jämsänkoski paper mill; KAU, Kaukas biopower plant.

Notes: [a] Since May 2022, CEM II has been replaced by CEM III/A in Nordkalk binders [63]; [b] ≥80% #0–0.2 mm and $\#_{max} < 2$ mm for CaO and LKD and $\#_{max} < 1.6$ mm for $Ca(OH)_2$ [18,64]; [c] JAM+CEM II, KAI+CEM II, and KAU+CEM II; [d] InfraStabi65 and InfraStabi80.

### *2.4. Stabilization tests in the laboratory*

For the test areas, stabilization tests were carried out in the laboratory prior to stabilization using clay and organic clay samples taken from the test areas and binders used in the test stabilizations. The stabilization tests were carried out in three laboratories as shown in Table 4. The number of stabilization test specimens is around 1130 in total [65]. The stabilization test results are presented in Section 3.

The strength determined by the stabilization tests depends on the procedure used to perform the stabilization tests (mixing, compaction, curing temperature, time, etc.) in addition to the properties of the soil to be stabilized and the binder recipe. The stabilization tests were carried out following the

guidelines of FTIA [12]. Before adding the binders, the soil samples were remolded and homogenized by mixing the soil carefully. The mixture for the stabilization test was made with a stand mixer with hook shaped mixer. The mixing time was set to 2–5 min. The diameter of the cylinder-shaped mold was 40–50 mm, and the height was 2 × diameter. The laboratories selected a compaction method (dynamic, rodding, and tapping), depending on the properties of the soil sample. "Dynamic" means compaction with a falling weight, "rodding" means tamping with a rod for each compaction layer, and "tapping" means knocking of the mold against a solid base [66].

**Table 3.** Binders and binder contents at the test stabilization sites (modified from [42]).

| **Test site** | T1 | T2 | T3 | T4 | T5 | T6 |
|---|---|---|---|---|---|---|
| **Binder** | Binder content, kg/m$^3$ = kg dry binder/m$^3$ soil | | | | | |
| KC20 | – | 70, 110 | – | – | | – |
| KC30 | – | – | – | – | 100–135, 135–170[c] | 100 |
| GREEN | 100–200[a], 80–160[b] | 70, 110 | 80, 120 | 80, 120, 160 | – | – |
| POZ | 100–200[a], 80–160[b] | – | 80, 102 | 80, 120, 160 | – | – |
| GTC2[a] | – | 70, 110 | 80, 120 | 80, 120 | 100–135, 135–170[c] | 100 |
| GTC3[a] | 100–200[a], 80–160[b] | 70, 110 | – | 120, 160 | – | – |
| CEM III/A, /B | 100–200[a], 80–160[b] | – | – | – | – | – |
| JAM+CEM II | – | – | 120, 160 | – | – | – |
| KAI+CEM II | – | – | 120, 160 | – | – | – |
| KAU+CEM II | 100–200[a], 80–160[b] | – | – | 120, 160 | – | – |
| Stabi65 | – | – | – | – | – | 100 |
| Stabi80 | – | – | 80, 120 | – | 100–135, 135–170[c] | – |

Notes: [a] Test areas S1 and S4: binder content, 150/120/100 kg/m$^3$ ("small") and 200/150/120 kg/m$^3$ ("big"); column top/middle/bottom, above +13 m (above sea level)/+13 to +9/+9 underneath. [b] Test area S6: binder content, 120/80 kg/m$^3$ ("small") and 160/120 kg/m$^3$ ("big"); column top/column bottom, above +11.5 m /+11.5 underneath. [c] Test area S1: binder content, 135/100 kg/m$^3$ ("small") and 170/135 kg/m$^3$ ("big"); column top/column bottom, above -12 m (under sea level)/-12 m underneath. Test area S2: 100 kg/m$^3$ ("small") and 135 kg/m$^3$ ("big"). Test area S3: 135/100 kg/m$^3$ ("small") and 170/135 kg/m$^3$ ("big"); above -10 m/-10 underneath.

### *2.5. Implementation of the test columns*

The test columns were implemented as separate contracts or in connection with a larger stabilization contract. The basic features of the implemented columns are as follows: Diameter, 0.6 or 0.7 m; column length, 5–20 m; target shear strength, 100–160 kPa; groundwater pressure level, 0–1 m below the ground surface; stabilization executed in 2019–2022. The curing of the test columns was examined with QC soundings. The number of the QC soundings in this study at the test fields is around 660 in total.

The implementation of the test columns was made according to the general code of practice for the construction of infrastructure [18]. In the general code, the rotation speed of the mixing tool is 100–

200 rpm during the withdrawal stage, and the withdrawal speed of the mixing tool (m/min) must be such that 200–250 blade rotations (r/m-column) are realized. For example, when using a mixing tool with three blade levels, the maximum withdrawal speed of the mixing tool is no more than 15 mm/rotation. The air pressure for binder injection should be as small as possible.

**Table 4.** Laboratories that carried out stabilization tests on clay and organic clay samples from test areas T1–T6 with different binders. A, Aalto University; N, Nordkalk Oy; R, Ramboll Finland Oy (modified from [55]).

| Test site / Binder | T1 | T2 | T3 | T4 | T5 | T6 | Tests pcs. |
|---|---|---|---|---|---|---|---|
| Calcareous binders | | | | | | | |
| KC20 | – | R | – | – | – | – | 105 |
| KC30 | – | R | N | – | R | R | |
| GREEN | N | R | N | N | – | – | 128 |
| POZ | N | – | N | N | – | – | 109 |
| Gypsum-containing binders | | | | | | | |
| GTC2 | – | R | N | N | R | R | 154 |
| GTC3 | N | – | – | – | – | – | 75 |
| Blast furnace slag binders | | | | | | | |
| CEM III/A | A, N, R | – | – | – | – | – | 79 |
| CEM III/B | R | – | – | – | – | – | 80 |
| FA containing binders | | | | | | | |
| KAI+CEM II 7:3 | – | – | R | – | – | – | 47 |
| JAM+CEM II 7:3 | A | – | R | N | – | – | 126 |
| KAU+CEM II 7:3 | A | – | – | A | – | – | 111 |
| Stabi65 | – | – | – | – | – | R | 117 |
| Stabi80 | – | R | R | N | R | – | |
| | Total stabilization tests: | | | | | | 1131 |

### *2.6. Overview of QC soundings*

This study is based on the results of the CP test (Figure 4), which is the most commonly employed quality sounding method in the Nordic countries, with some country-specific variants. The intent of the CP test is to measure the shear strength of stabilized soil indirectly from its penetration resistance. The tip of the penetrometer is compressed into the stabilized soil, and the force needed to penetrate the soil is measured from the surface end of the sounding tip. The measurement of static penetration resistance is continuous at 0.04 m intervals. The measured penetration resistance is converted into shear strength by dividing it by the bearing resistance factor $N_c$ = 10–15 (Equation 2), which has been calibrated by a vane penetrometer. When the strength of stabilized soil is excessively high for static penetration ($s_u >\approx$ 200 kPa), the methodology is shifted to dynamic penetration, in which case the blow count per 0.20 m is counted. The process is much like that of the dynamic probing or standard penetration test. Conversion of blows into static pushing resistance is represented by an empirical equation (Equation 3) [42,67,68].

$$s_u = \frac{(p-\sigma_0)}{Nc}, \tag{2}$$

$$\frac{10\ blows}{0.2\ m} => p_{blow} = 1000\ kPa, \tag{3}$$

where $s_u$ is the undrained shear strength of the soil mix (kPa); $p$ is the pushing resistance (kPa), i.e. the ratio of force $F$ required for pushing to tip area A (100 cm$^2$); $\sigma_0$ is the effective vertical stress in the soil (kPa); $N_c$ is the empirical coefficient (no units); and $p_{blow}$ is blow count per 0.20 m as static pushing resistance (kPa).

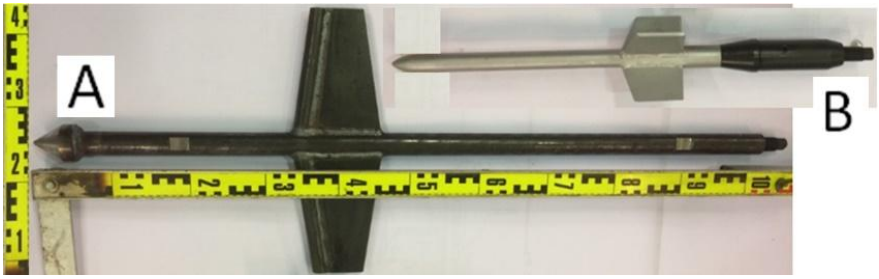


**Figure 4.** Column (A, "PK2/100") and vane penetrometer (B, "PS130/65") for columns. A: Tip underside area = 100 cm$^2$ and width −375 mm. B: Width −130 mm and height −65 mm [58].

*2.7. Variability in the shear strength of soil mixes in the laboratory and in the field*

The strength of stabilized soil is affected by many factors such as the soil properties, the type and content of binder, the mixing degree, and the curing conditions [69]. The mixing conditions and curing conditions are quite different from the standard laboratory mixing test. Usually, the field-stabilized soil column has a lower average strength and a larger strength deviation than the laboratory-stabilized soil [13]. Regarding shear strength testing of laboratory or in situ stabilized columns, the variability in the test results is mainly affected by three components: (1) The inherent variability of the properties of the natural soil [41] and binder, (2) the binder injection and mixing process, and (3) measurement error in UCS tests or QC soundings.

The variability in the undrained shear strength of natural Finnish clays has been estimated to be in the range of 0.10–0.30 [70,71]. When soil is stabilized in the laboratory, the heterogeneity decreases. Swedish studies have reported the COV to be 0.05–0.07 via laboratory tests of soil mixes, and Finnish studies have reported 0.04–0.07 [71–73]. Meanwhile, when soil is in situ stabilized, the heterogeneity increases. The FWHA guideline presents the COV of the in situ soil mix to be about double that of the COV = 0.13–0.40 of natural clay deposits. The COV of the soil mixes is 0.34–0.79 ($COV_{av.}$ = 0.56) according to the compression test results (UCS) of 7873 column samples from 10 deep stabilization projects [15]. According to Kitazume and Terashi [13], COV is 0.50–0.68 for the dry on-land stabilization method in Japan. The development of binders, Deep mixing (DM) machinery, and construction procedures have improved the quality of the soil mix and the COV of soil mixes nowadays by about 0.25 to 0.5 [74].

In the case of field strength, the QC sounding tip has been found to affect the value of COV. In a study on mass stabilized soil, it was found that COV based on soundings with a large surface tip, namely PK2/100, was smaller (0.08–0.67, average = 0.33) and with smaller tips (PA50 and CPT), COV was larger at 0.41–0.87 (average = 0.72; $A_{tip}$, 100, 50, and 16 $cm^2$) [68,75]. Bergman et al. [76] investigated the variation in strength of stabilized columns using cone penetration tests (CPTs) and found COV to be 0.11–0.37 (average = 0.23), while the CP COV was 0.07–0.25 (average = 0.14). In general, CPT tips are too small in relation to the column segment to represent the strength of the whole column's cross-section. A larger tip averages the sounding resistance and reduces the COV value. Al-Naqshabandy et al. [77] reported the COV of lime cement columns to be 0.3–0.55. The sounding method has also been found to influence the COV value. Wong et al. [78] investigated lime cement columns with CP soundings and FOPS tests. The study found that COV is 0.60 with CP tests and 0.86 with FOPS tests. Timoney [18] studied laboratory-compacted stabilized cement mini columns with PORT and PIRT, finding that with the PORT method, the COV was 0.09–0.16, and with PIRT, it was 0.06–0.13. Hov et al. [79] studied laboratory-compacted stabilized cement mini columns with PIRT, and the COV was 0.07–0.17. Both these COV value ranges are significantly smaller than those in full-scale in situ columns, indicating the effect of variation and the layered structure of natural soil. The effect of the binder injection and mixing effort, which usually increases the COV values, do not contribute to the variability.

Savila et al. [21] investigated the strength of cores taken from stabilized columns using UCS tests. The curing time of the columns was from 50 days to 3.5 years. According to the test results, the COV of calcareous binders was 0.12–0.42 (average = 0.26); for gypsum-containing binders, it was 0.40–0.65 (average = 0.53); for BFS-containing binders, it was 0.22–0.61 (average = 0.43); and for ash-containing binders, it was 0.42 (only one series of parallel samples). The test results did not show a significant correlation between the stabilized soil's strength and COV values. Forsman et al. [42] studied the variation in strength determined by QC soundings at six test stabilization sites with different types of binder mixtures. According to the test results, the COV of calcareous binders was 0.18–0.64 (average = 0.36); for gypsum-containing binders, it was 0.14–0.65 (average = 0.33); for BFS-containing binders, it was 0.26–0.79 (average = 0.48); and for ash-containing binders, it was 0.17–0.56 (average = 0.33). According to the extensive data, the water content, the shear strength of natural clay, and the curing time do not affect the COV for any of the four binder types considered. The effect of the strength of soil mixes and number of observations (sample size) seems to have some minor effect on the COV, and the effect varies slightly by binder type. All the COV values of the abovementioned tests are summarized in Figure 5.

Earlier studies (e.g. [21,80,81]) have found that the variation in the strength (COV) of stabilization tests and cored specimens follow a log-normal distribution. Navin and Filz [82] studied dataset of 2672 pcs. of UCS tests from six sites and stated that the DMM strength data tends to fit a log-normal distribution better than a normal distribution, a uniform distribution, or a triangular distribution Piispanen [75] observed that the variation (COV) in the strength of soil mix QC soundings indeed followed a log-normal distribution. Forsman et al. [42] observed that alongside the strength values, COV values defined from QC sounding data also follow a log-normal distribution. For the QC soundings of six test stabilization sites, the binder type-specific key statistics for the determined log-normal distributions are as follows:

- $COV_{5\%}$ = 0.14–0.18 and $COV_{95\%}$ = 0.60–0.64 are of the same magnitude for binder types containing lime, gypsum, and ash;
- $COV_{5\%}$ = 0.26 and $COV_{95\%}$ = 0.79 for BFS-containing binder type;
- In general, the mode value (the greatest likelihood) is in the range of COV = 0.2–0.4.

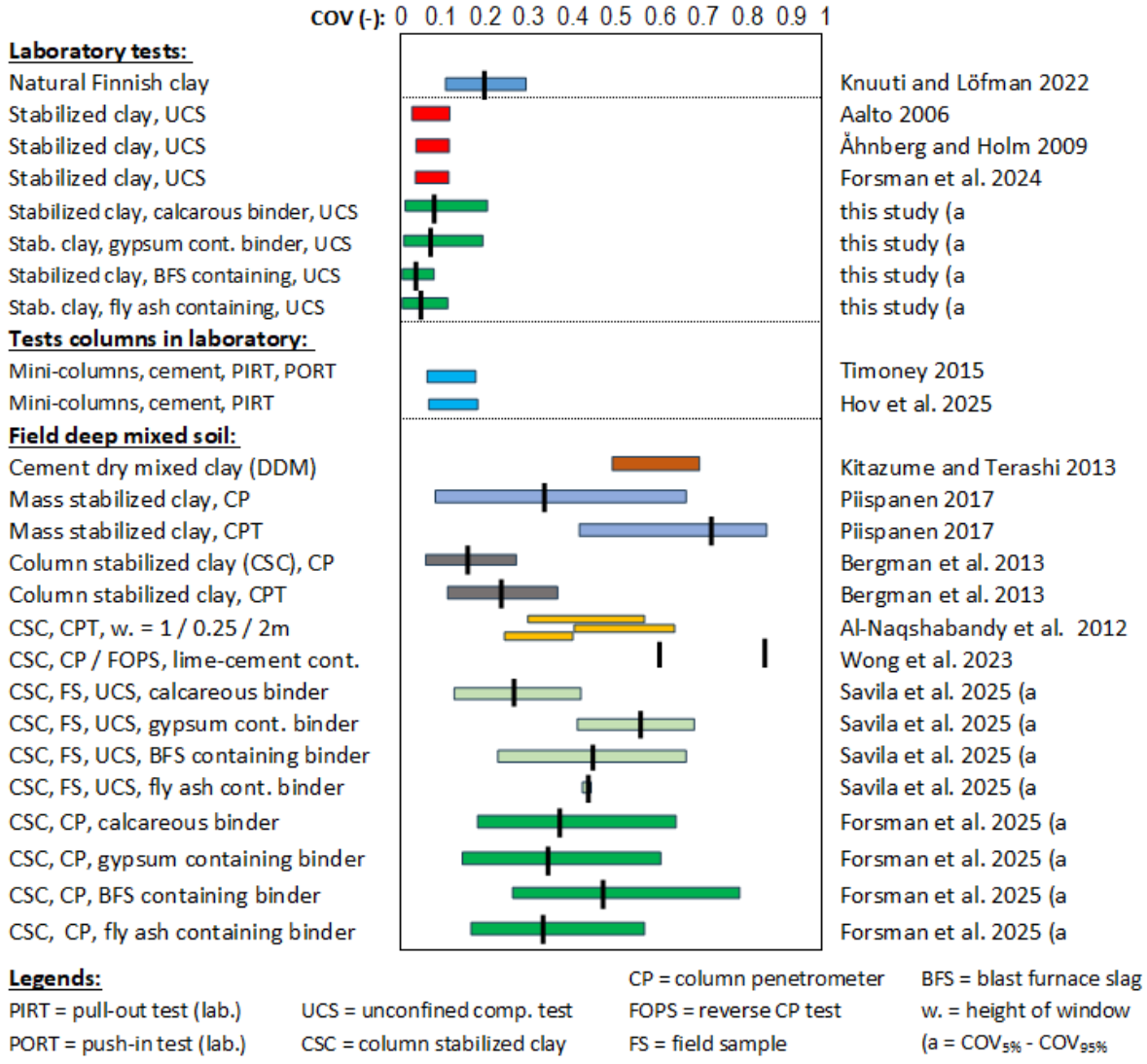


**Figure 5.** The COV values for soil mixes in laboratory and field studies. The black vertical line is the average value.

*2.8. Estimating the variability in the stabilization test results*

In this study, the COV was calculated using two estimation methods from the standard deviation. If there were at least three parallel test results, the COV for the stabilization test results was calculated using the samples' standard deviation (Equation 4)

$$SD = \sqrt{\frac{1}{n-1}\sum_{i=1}^{n}(x_i - \bar{x})^2}\,, \tag{4}$$

where $n$ is the number of observations used to calculate the arithmetic mean (average) $\bar{x}$. COV is then simply given as $SD/\bar{x}$.

For $n < 3$, SD was not calculated. It is evident that with such small number of test specimens, the statistical uncertainty in the defined sample's standard deviation becomes significant. Therefore, another estimation method for SD was used alongside the sample's SD. In this approximation method, the sample range $x_{max}–x_{min}$ is used to assess the variation in a small number of tests. If the data are normally distributed, Equation 5 can be used to obtain an estimate of the standard deviation $\hat{s}_x$ [83–85]

$$\hat{s}_x = N_n \times (x_{max} - x_{min}), \tag{5}$$

where $N_n$ is a multiplier, which is based on the number of data $n$ ($N_n$ = 0.886 for $n$ = 2, 0.510 for $n$ = 3, 0.486 for $n$ = 4, 0.430 for $n$ = 5, and 0.395 for $n$ = 6).

### *2.9. Transformation uncertainty in estimating the field to laboratory strength ratios*

The nomograms were derived by fitting them to the data regression functions, where laboratory shear strength $\tau_{lab}$ is used as a predictor to estimate the field to laboratory strength ratio $k_{F/L}$. Such regression functions are typically characterized by transformation uncertainty [41], since there is data scatter around the trendline. The amount of transformation uncertainty can be quantified using the error term $\varepsilon_i$ defined by Equation 6 [86]:

$$\varepsilon_i = \frac{observed\ k_{F/L}}{predicted\ k_{F/L}}, \tag{6}$$

where the predicted $k_{F/L}$ value is the factor given by the trendline with the observed value of laboratory shear strength (which was used to calculate observed value of $k_{F/L}$) as input. The average value of $\varepsilon_i$ error terms is the model bias ($b$), and the SD of $\varepsilon_i$ is then used to calculate the COV value of transformation uncertainty, denoted $\delta$ [86]. The bias $b$ should be close to 1, when the same dataset is used to fit the trendline and to estimate the transformation uncertainty (i.e., the regression curve should be unbiased).

This transformation uncertainty $\delta$ was then used to define a cautious estimate of the trendline, following the concept of characteristic values in the Eurocodes. Schneider has proposed an approximation function to derive a statistically defined characteristic value $X_k$, given by Equation 7 [87]:

$$X_k = \bar{x}\,(1 - 0.5 \times \mathrm{COV}), \tag{7}$$

which corresponds to a cautious mean when smaller value of the geotechnical property in question is unfavorable in the considered limit state (if a larger value is unfavorable, the minus sign is replaced with plus sign). The method provides an approximation of the 5% percentile of the sample mean's probability distribution, which corresponds to the 31% percentile of the underlying point value distribution (the sample's mean has smaller standard deviation than the point values). Equation 7 was used to determine the characteristic trendline by using the trendline value as $\bar{x}$ and the transformation uncertainty $\delta$ as the COV.

To validate the characteristic trendlines, a Monte Carlo simulation was performed while assuming average variability (COV) for the laboratory and field shear strength values. At the given laboratory strength values ($\tau_{lab}$), 100,000 random values were generated from the log-normal distribution while

assuming the average observed COV values. Next, the same number of $\tau_{field}$ values was generated by assuming the mean value to be equal to the trendline's prediction, and COV was taken as the average observed for $\tau_{field}$ for the same binder type (see Figure 5). The $k_{F/L}$ values were then calculated using the generated samples. The 31% percentiles of the generated samples were derived and plotted next to the characteristic trendlines based on Equation 7. Good agreement between the percentiles was taken as an indication of Equation 7 providing reasonable results.

## 3 Results

### *3.1. Stabilization test results*

A summary of the stabilization test results examined in this study is presented in Table 5. A complete collection of the stabilization test results can be found in Tables 6–13. All the binders achieved reasonable strengths, on the basis of which it is possible to select and optimize the amount of binder for stabilization during production. In Tables 7–13, the average compression strength is presented as the average of two or three parallel specimens' UCS results. The single compression test strengths are also presented. The summarizing table roughly shows the effect of the content of different binders with clay from six test sites on the strength achieved. The results show that the greatest compression strengths were achieved with CEM III binders. The lowest strengths were achieved with FA+CEM II 7:3 mixtures, where the ash is directly from the silo and the dry ash is mixed with cement at the test site. In the InfraStabi binders, FA is activated with a pin mill, thus resulting in higher strengths compared with the FA+CEM II mixture. In the following sections of this article, the results of the stabilization test are presented as shear strengths ($\tau_{lab} = \sigma_{UCS}/2$) instead of compression strength.

### *3.2. Variation in the stabilization test results (COV and $\hat{s}_x$/avg)*

A statistical analysis of the stabilization test results has been carried out. The effect of the strength achieved in the stabilization tests on the COV value has been examined with the help of Figure 6. The figure has been prepared for different binder types, and they present a combination of the results from test sites T1–T6. The COV values shown in the figure have been determined from the results of three parallel compression tests. According to the results, COV is clearly higher for calcareous and gypsum-containing binder types than for BFS- and FA-containing binder types.

The figure also shows linear trendlines which have been fitted to the data representing either 28 d or 91 d of curing time. According to the trendlines, the achieved shear strength does not significantly affect the COV value. The curing time of binders containing BFS and ash does not significantly affect the COV values' trendline. With calcareous and gypsum-containing binders, the slopes of the trendlines for samples cured for 28 d and 91 d differ from each other; However, there is no clear indication that the curing time influences the COV value.

**Table 5.** Compression strengths (UCS) achieved with different binders and contents in stabilization tests with clay and organic clay samples from test sites T1–T6. Curing time: 91 d.

| Binder type and binder | 70–105 kg/m$^3$ | | 110–145 kg/m$^3$ | | 150–200 kg/m$^3$ | |
|---|---|---|---|---|---|---|
| Calcareous binders | Min–max | Avg | Min–max | Avg | Min–max | Avg |
| KC20 and KC30 | 381–1150 | 698 | 333–1775 | 766 | 777–1070 | 923 |
| GREEN | 291–682 | 422 | 184–1315 | 547 | 239–1540 | 624 |
| POZ | 234–345 | 302 | 96–451 | 291 | 114–518 | 228 |
| Gypsum-containing binders | | | | | | |
| GTC2 | 364–531 | 448 | 366–884 | 595 | 377–770 | 588 |
| GTC3 | 217–592 | 386 | 311–1030 | 603 | 588–1375 | 1003 |
| BFS-containing binders | | | | | | |
| CEM III/A | 859–1347 | 1121 | 1107–2713 | 1617 | 1687–2623 | 2152 |
| CEM III/B | 414–899 | 698 | 671–2067 | 1219 | 1270–2960 | 1967 |
| FA-containing binders | | | | | | |
| JAM+CEM II | 119–188 | 148 | 58–333 | 152 | 93–230 | 159 |
| KAU+CEM II | 129–171 | 144 | 113–423 | 204 | 183–548 | 285 |
| InfraStabi65 and 80 | 125–596 | 366 | 184–1055 | 604 | 558–999 | 779 |

**Table 6.** Stabilization tests. Average variability (COV and $\hat{s}_x$/avg) of the $\tau_{lab}$ of soil mixes stabilized with different binder types and binders. Clay samples are from test sites T1–T6.

| Binder content | 28 d | | 91 d | | 28 d + 91 d | |
|---|---|---|---|---|---|---|
| | $COV_{av}$ [a] | $\hat{s}_x$/avg [b] | $COV_{av}$ | $\hat{s}_x$/avg | $COV_{av}$ | $\hat{s}_x$/avg |
| Calcareous binders | **0.09** | **0.08** | **0.09** | **0.09** | **0.09** | **0.09** |
| KC20 and KC30 | 0.10 | 0.06 | 0.09 | 0.07 | 0.10 | 0.07 |
| GREEN | 0.07 | 0.10 | 0.12 | 0.11 | 0.09 | 0.10 |
| POZ | 0.09 | 0.08 | 0.07 | 0.09 | 0.08 | 0.09 |
| Gypsum-containing binders | **0.08** | **0.07** | **0.10** | **0.09** | **0.09** | **0.08** |
| GTC3 | 0.09 | 0.06 | 0.09 | 0.11 | 0.09 | 0.07 |
| GTC2 | 0.08 | 0.08 | 0.11 | 0.08 | 0.10 | 0.09 |
| BFS-containing binders | **0.04** | **0.04** | **0.04** | **0.04** | **0.04** | **0.04** |
| CEM III/A | 0.04 | 0.03 | 0.03 | 0.04 | 0.04 | 0.03 |
| CEM III/B | 0.04 | 0.04 | 0.04 | 0.05 | 0.04 | 0.04 |
| FA-containing binders | **0.07** | **0.05** | **0.03** | **0.04** | **0.05** | **0.05** |
| JAM+CEM II | 0.05 | 0.04 | 0.04 | 0.05 | 0.05 | 0.04 |
| KAI+CEM II | – | 0.05 | – | – | – | – |
| KAU+CEM II | 0.05 | 0.05 | 0.02 | 0.02 | 0.03 | 0.04 |
| InfraStabi65 and 80 | 0.11 | 0.06 | 0.03 | 0.06 | 0.07 | 0.06 |

Note: [a] 3 pcs. = COV based on three parallel stabilization tests (UCS); [b] 2-3 pcs. = $\hat{s}_x$/avg (see Equation 5)

The curing time does not seem to affect the average COV values either, as shown in Table 6. The

table presents the COV values for all the binders tested. The COV values are shown in Table 6 for specimens cured for 28 d, 91 d, and 28 + 91 d. In the analysis, COV was determined for the test results, based on the results of three parallel compression tests. In addition, $\hat{s}_x$/avg was determined for test results, based on the results of three and two parallel tests. The values of $\hat{s}_x$ and $\hat{s}_x$/avg, based on Equations 4 and 5, are presented in Tables 7–13. Calculated values of $\hat{s}_x$ are presented for $n$ = 2–3.

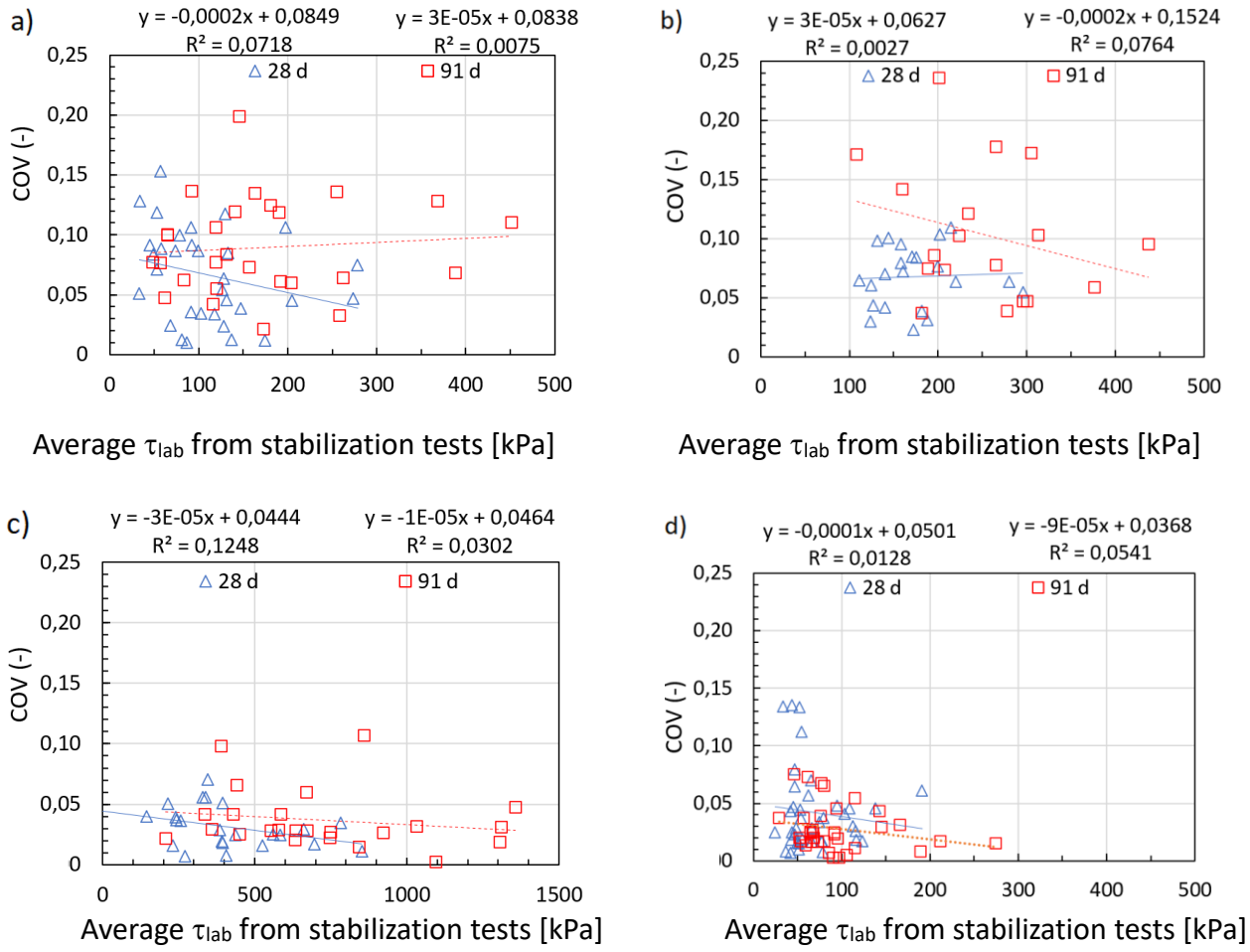


**Figure 6.** Average $\tau_{lab}$ from stabilization tests and COV for different binder types: (a) Calcareous, (b) gypsum-containing, (c) BFS-, and (d) FA-containing binders. Clay samples are from test sites T1–T6. Each marker represents the COV value for three parallel UCS test results.

For the calcareous and gypsum-containing binder types, the $COV_{av}$ values (28 + 91 d) are 0.08–0.10. The $COV_{av}$ values are 0.04 for BFS-containing binders and 0.03–0.07 for FA-containing binders. Correspondingly, the $\hat{s}_x$/mean values are 0.07–0.09 for the calcareous and gypsum-containing binders and 0.04 for BFS-containing binders and 0.04–0.05 for FA-containing binders. The $COV_{av}$ ($SD$/avg) and $\hat{s}_x$/avg values do not differ significantly (mainly 0–0.01). According to this evaluation, it appears that $\hat{s}_x$/avg is a reasonable method for estimating the variation in the results of stabilization tests with a small $n$ (two or three specimens). The $COV_{av}$ values are highest for the binders KC20, KC30, GREEN, POZ, GTC2, and GTC3 and the $COV_{av}$ values are lowest for the binders CEM III/A, CEM III/B, JAM FA+CEM II, and KAU FA+CEM II. The $COV_{av}$ of the binders Stabi65 and Stabi80 is in between the values above. In the

literature, $COV_{av}$ has been reported to be 0.04–0.07 for stabilization test results (see Section 2.7). The COV values for BFS- and FA-containing binders presented in this study fall within the same range. For binders containing lime and gypsum, the variation is slightly greater than that presented in the literature.

**Table 7.** Stabilization test results for the binders KC20 and KC30, and COV values for the results of three parallel compression tests. Values for $\hat{s}_x$/avg (Equation 5) were based on the results of two and three parallel tests. Curing time: 28 d and 91 d.

| | | Curing time 28 d | | | | | | | Curing time 91 d | | | | | | |
|---|---|---|---|---|---|---|---|---|---|---|---|---|---|---|---|
| Binder | Dosage | Compression | | | avg | STD | COV | $s_x$/avg | Compression | | | avg | STD | COV | $s_x$/avg |
| Site | (kg/m$^3$) | strength (kPa) | | | (kPa) | (kPa) | ( - ) | ( - ) | strength (kPa) | | | (kPa) | (kPa) | ( - ) | ( - ) |
| KC20 | 70 | 468 | 491 | - | 480 | - | - | 0.04 | 903 | 928 | - | 916 | - | - | 0.02 |
| **site T2** | 150 | 697 | 601 | - | 649 | - | - | 0.13 | 1070 | 1070 | - | 1070 | - | - | 0.00 |
| | 70 | 431 | 473 | - | 452 | - | - | 0.08 | 839 | 868 | - | 854 | - | - | 0.03 |
| | 110 | 614 | 559 | - | 587 | - | - | 0.08 | 1000 | 1050 | - | 1025 | - | - | 0.04 |
| | 70 | 509 | 506 | - | 508 | - | - | 0.01 | 1280 | 1020 | - | 1150 | - | - | 0.20 |
| | 110 | 845 | 731 | - | 788 | - | - | 0.13 | 1520 | 2030 | - | 1775 | - | - | 0.25 |
| KC30 | 70 | 424 | 430 | - | 427 | - | - | 0.01 | 538 | 642 | - | 590 | - | - | 0.16 |
| **site T2** | 150 | 501 | 564 | - | 533 | - | - | 0.10 | 706 | 834 | 790 | 777 | 53.1 | 0.07 | 0.08 |
| | 70 | 371 | 370 | - | 371 | - | - | 0.00 | 464 | 501 | - | 483 | - | - | 0.07 |
| | 110 | 576 | 588 | - | 582 | - | - | 0.02 | 791 | 771 | - | 781 | - | - | 0.02 |
| KC30 | 135 | 212 | 212 | - | 212 | - | - | 0.00 | 326 | 339 | - | 333 | - | - | 0.03 |
| **site T5** | 135 | 501 | 455 | - | 478 | - | - | 0.09 | 845 | - | - | - | - | - | - |
| | 170 | 736 | 669 | - | 703 | - | - | 0.08 | 1200 | - | - | - | - | - | - |
| | 135 | 280 | 310 | - | 295 | - | - | 0.09 | 476 | 465 | - | 471 | - | - | 0.02 |
| | 135 | 574 | 616 | - | 595 | - | - | 0.06 | 855 | - | - | - | - | - | - |
| | 170 | 787 | 804 | - | 796 | - | - | 0.02 | 1090 | - | - | - | - | - | - |
| | 135 | 363 | 336 | - | 350 | - | - | 0.07 | 548 | 553 | - | 551 | - | - | 0.01 |
| | 135 | 786 | 791 | - | 789 | - | - | 0.01 | 1190 | 1190 | - | 1190 | - | - | 0.00 |
| | 135 | 195 | 194 | - | 195 | - | - | 0.00 | 368 | 355 | - | 362 | - | - | 0.03 |
| KC30 | 80 | 298 | 250 | 250 | 266 | 27.7 | 0.10 | 0.09 | - | - | - | | | | - |
| **site T3** | 120 | 448 | 395 | 345 | 396 | 51.5 | 0.13 | 0.13 | 531 | 563 | 481 | 525 | 33.7 | 0.06 | 0.08 |
| | 80 | 272 | 263 | 234 | 256 | 19.9 | 0.08 | 0.08 | 412 | 414 | 317 | 381 | 45.3 | 0.12 | 0.13 |
| | 80 | - | 359 | 396 | 378 | - | - | 0.09 | - | - | - | - | - | - | - |
| | 120 | 578 | 596 | - | 587 | - | - | 0.03 | 593 | 700 | - | 647 | - | - | 0.15 |
| | 80 | 305 | 264 | - | 285 | - | - | 0.13 | 495 | 518 | 536 | 516 | 16.8 | 0.12 | 0.04 |
| KC30 | 100 | - | 301 | 304 | 303 | - | - | 0.01 | - | - | - | - | - | - | - |
| **site T6** | 120 | - | 378 | 370 | 374 | - | - | 0.02 | - | - | - | - | - | - | - |
| | 140 | - | 404 | 435 | 420 | - | - | 0.07 | - | - | - | - | - | - | - |
| KC20 + KC30 | | | | | avg. | 33.0 | 0.10 | 0.06 | | | | avg. | 37.2 | 0.09 | 0.07 |
| av. 28 and 91 d | | | | | avg. | 35.1 | 0.10 | 0.07 | | | | | | | |

**Table 8.** Stabilization test results for the binder GREEN and COV values for the results of three parallel compression tests. Values for $\hat{s}_x$/avg (Equation 5) were based on the results of two and three parallel tests. Curing time: 28 d and 91 d.

| | | Curing time 28 d | | | | | | | Curing time 91 d | | | | | | |
|---|---|---|---|---|---|---|---|---|---|---|---|---|---|---|---|
| Binder | Dosage | Compression | | | avg | STD | COV | $s_x$ /avg | Compression | | | avg | STD | COV | $s_x$ /avg |
| Site | (kg/m$^3$) | strength (kPa) | | | (kPa) | (kPa) | ( - ) | ( - ) | strength (kPa) | | | (kPa) | (kPa) | ( - ) | ( - ) |
| GREEN | 120 | 166 | 207 | 182 | 185 | 20.7 | 0.11 | 0.11 | 262 | 328 | 253 | 281 | 33.4 | 0.12 | 0.14 |
| **site T1** | 150 | 279 | 273 | 271 | 274 | 4.2 | 0.02 | 0.01 | - | 335 | 323 | 329 | - | - | 0.03 |
| | 100 | 344 | 350 | 354 | 349 | 5.0 | 0.01 | 0.01 | - | 414 | 431 | 423 | - | - | 0.04 |
| | 120 | 386 | 431 | 411 | 409 | 22.5 | 0.06 | 0.06 | 433 | 601 | 496 | 510 | 69.3 | 0.14 | 0.17 |
| | 150 | 132 | 139 | 139 | 137 | 4.0 | 0.03 | 0.03 | 242 | 260 | 215 | 239 | 18.5 | 0.08 | 0.10 |
| | 200 | - | 160 | 257 | 209 | - | - | 0.41 | 375 | - | 344 | 360 | - | - | 0.08 |
| | 120 | 179 | 176 | 191 | 182 | 7.9 | 0.04 | 0.04 | 236 | 272 | 210 | 239 | 25.4 | 0.11 | 0.13 |
| | 150 | 248 | 259 | 262 | 256 | 7.4 | 0.03 | 0.03 | 302 | 411 | 373 | 362 | 45.2 | 0.12 | 0.15 |
| | 100 | 375 | 410 | - | 393 | - | - | 0.03 | - | 416 | 444 | 430 | - | - | 0.06 |
| | 120 | 571 | 560 | 512 | 548 | 31.4 | 0.06 | 0.05 | - | 656 | 948 | 802 | - | - | 0.32 |
| | 120 | 192 | 132 | - | 162 | - | - | 0.33 | 276 | 255 | - | 266 | - | - | 0.07 |
| | 160 | 232 | 218 | - | 225 | - | - | 0.06 | 394 | 512 | - | 453 | - | - | 0.23 |
| | 80 | 218 | 271 | 290 | 260 | 37.3 | 0.14 | 0.14 | 370 | 365 | 417 | 384 | 23.4 | 0.06 | 0.07 |
| | 120 | 512 | 612 | 546 | 557 | 50.8 | 0.09 | 0.09 | 869 | 693 | 651 | 738 | 94.4 | 0.13 | 0.15 |
| GREEN | 120 | 137 | 139 | 165 | 147 | 15.6 | 0.11 | 0.10 | 158 | 218 | 176 | 184 | 25.1 | 0.14 | 0.17 |
| **site T4** | 160 | 162 | 179 | 209 | 183 | 23.8 | 0.13 | 0.13 | 292 | 258 | 239 | 263 | 21.9 | 0.08 | 0.10 |
| Green | 70 | - | 217 | 239 | 228 | - | - | 0.09 | - | 306 | 336 | 321 | - | - | 0.08 |
| **site T2** | 110 | - | 556 | - | - | - | - | - | - | 731 | 674 | 703 | - | - | 0.07 |
| | 150 | 853 | 855 | - | 854 | - | - | 0.00 | 1190 | 1140 | - | 1165 | - | - | 0.04 |
| | 70 | - | 264 | 220 | 242 | - | - | 0.16 | 245 | 373 | 256 | 291 | 58 | 0.20 | 0.22 |
| | 110 | - | 467 | - | - | - | - | - | - | 730 | 658 | 694 | - | - | 0.09 |
| | 150 | - | 826 | 726 | 776 | - | - | 0.11 | 991 | 764 | 954 | 903 | 99 | 0.11 | 0.13 |
| | 70 | - | 433 | 480 | 457 | - | - | 0.09 | - | 637 | 726 | 682 | - | - | 0.12 |
| | 110 | - | 774 | 804 | 789 | - | - | 0.03 | - | 1310 | 1320 | 1315 | - | - | 0.01 |
| | 150 | - | - | - | - | - | - | - | - | 1540 | 1540 | 1540 | - | - | 0.00 |
| GREEN | 120 | - | 358 | - | - | - | - | - | - | 428 | 407 | 418 | - | - | - |
| **site T3** | 150 | - | 553 | - | - | - | - | - | - | 735 | - | - | - | - | - |
| | 120 | - | 328 | 280 | 304 | - | - | 0.14 | - | 540 | 532 | 536 | - | - | - |
| GREEN | | | | | | 19.2 | 0.07 | 0.10 | | | | | 46.7 | 0.12 | 0.11 |
| av. 28 and 91 d | | | | | | 33.0 | 0.09 | 0.10 | | | | | | | |

**Table 9.** Stabilization test results for the binder POZ and COV values for the results of three parallel compression tests. Values for $\hat{s}_x$/avg (Equation 5) were based on the results of two and three parallel tests. Curing time: 28 d and 91 d.

| | | Curing time 28 d | | | | | | | Curing time 91 d | | | | | | |
|---|---|---|---|---|---|---|---|---|---|---|---|---|---|---|---|
| Binder | Dosage | Compression | | | avg | STD | COV | $s_x$ /avg | Compression | | | avg | STD | COV | $s_x$ /avg |
| Site | (kg/m$^3$) | strength (kPa) | | | (kPa) | (kPa) | ( - ) | ( - ) | strength (kPa) | | | (kPa) | (kPa) | ( - ) | ( - ) |
| POZ | 120 | 97 | 108 | 88 | 98 | 10.0 | 0.10 | 0.10 | 114 | 146 | 131 | 130 | 13.1 | 0.10 | 0.13 |
| **site T1** | 150 | 99 | 104 | 117 | 107 | 9.3 | 0.09 | 0.09 | 152 | 176 | 171 | 166 | 10.3 | 0.06 | 0.07 |
| | 100 | 170 | 173 | 174 | 172 | 2.1 | 0.01 | 0.01 | - | 250 | 218 | 234 | - | - | 0.12 |
| | 120 | 210 | 210 | 195 | 205 | 8.7 | 0.04 | 0.04 | 249 | 249 | 221 | 240 | 13.2 | 0.06 | 0.06 |
| | 150 | 56 | 68 | 77 | 67 | 10.5 | 0.16 | 0.16 | 122 | 132 | 118 | 124 | 5.9 | 0.05 | 0.06 |
| | 200 | 123 | 128 | 89 | 113 | 21.2 | 0.19 | 0.18 | 139 | 112 | 140 | 130 | 13.0 | 0.10 | 0.11 |
| | 120 | 70 | 68 | 62 | 67 | 4.2 | 0.06 | 0.06 | 95 | 87 | 105 | 96 | 7.4 | 0.08 | 0.10 |
| | 150 | 79 | 99 | 91 | 90 | 10.1 | 0.11 | 0.11 | 102 | 123 | 116 | 114 | 8.7 | 0.08 | 0.09 |
| | 100 | 258 | 252 | 280 | 263 | 14.7 | 0.06 | 0.05 | 281 | 386 | 312 | 326 | 44.0 | 0.13 | 0.16 |
| | 120 | 288 | 286 | 311 | 295 | 13.9 | 0.05 | 0.04 | 442 | 385 | 397 | 408 | 24.5 | 0.06 | 0.07 |
| | 120 | 126 | 140 | - | 133 | - | - | 0.09 | 222 | 184 | - | 203 | - | - | 0.17 |
| | 160 | 325 | 316 | - | 321 | - | - | 0.02 | 557 | 478 | - | 518 | - | - | 0.14 |
| | 80 | 234 | 265 | 260 | 253 | 16.6 | 0.07 | 0.06 | 336 | 346 | 354 | 345 | 7.4 | 0.02 | 0.03 |
| | 120 | 317 | 329 | - | 323 | - | - | 0.03 | 412 | 475 | - | 444 | - | - | 0.13 |
| POZ | 120 | 199 | 177 | 219 | 198 | 21.0 | 0.11 | 0.11 | 227 | 224 | 246 | 232 | 9.7 | 0.04 | 0.05 |
| **site T4** | 160 | 225 | 239 | 244 | 236 | 9.8 | 0.04 | 0.04 | 344 | 289 | 307 | 313 | 22.9 | 0.07 | 0.09 |
| | 120 | 104 | 129 | 115 | 116 | 12.5 | 0.11 | 0.11 | - | - | - | - | - | - | - |
| | 160 | 162 | 165 | 160 | 162 | 2.5 | 0.02 | 0.02 | - | - | - | - | - | - | - |
| | 120 | 89 | 113 | 118 | 107 | 15.5 | 0.15 | 0.14 | - | - | - | - | - | - | - |
| | 160 | 166 | 170 | 135 | 157 | 19.2 | 0.12 | 0.11 | - | - | - | - | - | - | - |
| POZ | 120 | - | 253 | 289 | 271 | - | - | 0.12 | - | 427 | 410 | 419 | - | - | 0.04 |
| **site T3** | 120 | - | 319 | 270 | 295 | - | - | 0.15 | - | 439 | 463 | 451 | - | - | 0.05 |
| POZ | | | | | | 11.9 | 0.09 | 0.09 | | | | | 15.0 | 0.07 | 0.09 |
| av. 28 and 91 d | | | | | | 13.4 | 0.08 | 0.08 | | | | | | | |
| KC20, KC30, GREEN, POZ | | | | | | **21.4** | **0.09** | **0.00** | | | | **0.09** | **33.0** | **0.09** | **0.09** |
| av. 28 and 91 d | | | | | | **27.2** | **0.09** | **0.09** | | | | | | | |

**Table 10.** Stabilization test results for the binders CTC3 (a) and GTC2 (b), and COV values for the results of three parallel compression tests. Values for $\hat{s}_x$/avg (Equation 5) were based on the results of two and three parallel tests. Curing time: 28 d and 91 d.

| **(a)** | | Curing time 28 d | | | | | | | Curing time 91 d | | | | | | |
|---|---|---|---|---|---|---|---|---|---|---|---|---|---|---|---|
| Binder | Dosage | Compression | | | avg | STD | COV | $s_x$ /avg | Compression | | | avg | STD | COV | $s_x$ /avg |
| Site | (kg/m$^3$) | strength (kPa) | | | (kPa) | (kPa) | ( - ) | ( - ) | strength (kPa) | | | (kPa) | (kPa) | ( - ) | ( - ) |
| GTC3 | 120 | 360 | 349 | 383 | 364 | 17.3 | 0.05 | 0.05 | 587 | 541 | 541 | 556 | 21.7 | 0.04 | 0.04 |
| **site T1** | 150 | 509 | 449 | - | 479 | - | - | 0.11 | 855 | - | 684 | 770 | - | - | 0.20 |
| | 100 | 386 | 360 | 384 | 377 | 14.5 | 0.04 | 0.04 | 384 | 479 | 483 | 449 | 45.8 | 0.10 | 0.11 |
| | 120 | 611 | 617 | 546 | 591 | 39.4 | 0.07 | 0.06 | 694 | 764 | 801 | 753 | 44.4 | 0.06 | 0.07 |
| | 150 | 241 | 253 | 268 | 254 | 13.5 | 0.05 | 0.05 | 361 | 417 | 354 | 377 | 28.2 | 0.07 | 0.09 |
| | 200 | 274 | 331 | 343 | 316 | 36.9 | 0.12 | 0.11 | 574 | 641 | 591 | 602 | 28.4 | 0.05 | 0.06 |
| | 120 | 252 | 323 | 289 | 288 | 35.5 | 0.12 | 0.13 | 335 | 536 | 335 | 402 | 94.8 | 0.24 | 0.26 |
| | 150 | 355 | 342 | 336 | 344 | 9.7 | 0.03 | 0.03 | - | 639 | 625 | 632 | - | - | 0.02 |
| | 100 | 312 | 333 | 381 | 342 | 35.4 | 0.10 | 0.10 | 543 | 575 | 476 | 531 | 41.2 | 0.08 | 0.10 |
| | 120 | 450 | 412 | 349 | 404 | 51.0 | 0.13 | 0.13 | 522 | 552 | 759 | 611 | 105.4 | 0.17 | 0.20 |
| | 120 | 263 | - | - | - | - | - | - | 391 | 341 | - | 366 | - | - | 0.12 |
| | 160 | 378 | 363 | - | 371 | - | - | 0.04 | 519 | 603 | - | 561 | - | - | 0.13 |
| | 80 | 291 | 309 | 351 | 317 | 30.8 | 0.10 | 0.10 | 380 | 364 | 347 | 364 | 13.5 | 0.04 | 0.05 |
| | 120 | 587 | 510 | 583 | 560 | 43.3 | 0.08 | 0.07 | 935 | - | 832 | 884 | - | - | 0.10 |
| GTC3 | | | | | | 29.8 | 0.08 | 0.08 | | | | | 47.0 | 0.09 | 0.11 |
| av. 28 and 91 d | | | | | | 38.4 | 0.09 | 0.09 | | | | | | | |
| **b)** | | | | | | | | | | | | | | | |
| GTC2 | 80 | 182 | 237 | - | 210 | | | 0.23 | 266 | 209 | 176 | 217 | 37.2 | 0.17 | 0.21 |
| **site T4** | 120 | 270 | 297 | 275 | 281 | 14.4 | 0.05 | 0.05 | 459 | 541 | 403 | 468 | 56.7 | 0.12 | 0.15 |
| GTC2 | 70 | - | 174 | 170 | 172 | - | - | 0.02 | - | 229 | 221 | 225 | - | - | 0.03 |
| **site T2** | 110 | - | 531 | - | - | - | - | - | - | 648 | 657 | 653 | - | - | 0.01 |
| | 150 | 825 | 841 | - | 833 | - | - | 0.02 | 1180 | 1170 | - | 1175 | - | - | 0.01 |
| | 70 | - | 270 | 259 | 265 | - | - | 0.04 | 323 | 335 | - | 329 | - | - | 0.03 |
| | 110 | - | - | 421 | - | - | - | - | - | 602 | 551 | 577 | - | - | 0.08 |
| | 150 | - | 777 | 753 | 765 | - | - | 0.03 | 758 | 920 | 947 | 875 | 83.5 | 0.10 | 0.11 |
| | 70 | - | 342 | 342 | 342 | - | - | 0.00 | - | 469 | 445 | 457 | - | - | 0.05 |
| | 110 | - | 570 | 542 | 556 | - | - | 0.04 | - | 1020 | 1040 | 1030 | - | - | 0.02 |
| | 150 | - | - | - | - | - | - | - | - | 1450 | 1300 | 1375 | - | - | 0.10 |
| GTC2 | 135 | - | 437 | 433 | 435 | - | - | 0.01 | - | 548 | 541 | 545 | - | - | 0.01 |
| **site T5** | 100 | - | 378 | 365 | 372 | - | - | 0.03 | - | 429 | - | - | - | - | - |
| | 135 | - | 714 | 732 | 723 | - | - | 0.02 | - | 795 | - | - | - | - | - |
| | 170 | - | 815 | 826 | 821 | - | - | 0.01 | - | 1070 | - | - | - | - | - |
| | 100 | - | 413 | 404 | 409 | - | - | 0.02 | - | 567 | 550 | 559 | - | - | 0.03 |
| | 135 | - | 627 | 619 | 623 | - | - | 0.01 | - | 929 | 891 | 910 | - | - | 0.04 |

*Continued on next page*

| (b) | | Curing time 28 d | | | | | | | Curing time 91 d | | | | | | |
|---|---|---|---|---|---|---|---|---|---|---|---|---|---|---|---|
| Binder | Dosage | Compression | | | avg | STD | COV | $s_x$ /avg | Compression | | | avg | STD | COV | $s_x$ /avg |
| Site | (kg/m$^3$) | strength (kPa) | | | (kPa) | (kPa) | ( - ) | ( - ) | strength (kPa) | | | (kPa) | (kPa) | ( - ) | ( - ) |
| | 100 | - | 365 | 372 | 369 | - | - | 0.02 | - | 412 | - | - | - | - | - |
| | 135 | - | 637 | 651 | 644 | - | - | 0.02 | - | 733 | - | - | - | - | - |
| | 170 | - | 689 | 689 | 689 | - | - | 0.00 | - | 881 | - | - | - | - | - |
| | 100 | - | 327 | 351 | 339 | - | - | 0.06 | - | 492 | 460 | 476 | - | - | 0.06 |
| | 135 | - | 470 | 446 | 458 | - | - | 0.05 | - | 708 | 717 | 713 | - | - | 0.01 |
| | 135 | - | 641 | 655 | 648 | - | - | 0.02 | - | 728 | 741 | 735 | - | - | 0.02 |
| | 135 | - | 402 | 405 | 404 | - | - | 0.01 | - | 640 | 653 | 647 | - | - | 0.02 |
| GTC2 | 120 | 344 | 344 | - | 344 | - | - | 0.00 | 430 | - | - | - | - | - | - |
| **site T3** | 150 | 337 | 267 | - | 302 | - | - | 0.21 | 617 | 558 | - | 588 | - | - | 0.09 |
| | 120 | 313 | 390 | - | 352 | - | - | 0.19 | 400 | 418 | - | 409 | - | - | 0.04 |
| | 80 | 235 | 298 | 259 | 264 | 31.8 | 0.12 | 0.12 | - | - | - | - | - | - | - |
| | 120 | 353 | 314 | 386 | 351 | 36.0 | 0.10 | 0.10 | 400 | 458 | 388 | 415 | 30.6 | 0.07 | 0.09 |
| | 80 | 257 | 239 | 247 | 248 | 9.0 | 0.04 | 0.04 | 357 | 437 | 380 | 391 | 33.6 | 0.09 | 0.10 |
| | 80 | 277 | 243 | - | 260 | - | - | 0.12 | - | - | - | - | - | - | - |
| | 120 | 295 | 294 | 253 | 281 | 24.0 | 0.09 | 0.08 | 266 | 356 | - | 311 | - | - | 0.26 |
| | 80 | 438 | 394 | 364 | 399 | 37.2 | 0.09 | 0.09 | - | - | - | - | - | - | - |
| | 120 | 473 | 405 | 443 | 440 | 34.1 | 0.08 | 0.08 | 569 | 595 | 717 | 627 | 64.5 | 0.10 | 0.12 |
| | 80 | 331 | 289 | 343 | 321 | 28.4 | 0.09 | 0.09 | 565 | 581 | 630 | 592 | 27.7 | 0.05 | 0.06 |
| | 80 | 242 | 208 | 217 | 222 | 17.6 | 0.08 | 0.08 | - | - | - | - | - | - | - |
| | 120 | 400 | 393 | 496 | 430 | 57.6 | 0.13 | 0.12 | 492 | 661 | 440 | 531 | 94.3 | 0.18 | 0.21 |
| | 80 | 234 | 270 | 245 | 250 | 18.4 | 0.07 | 0.07 | 384 | 288 | 288 | 320 | 45.3 | 0.14 | 0.15 |
| GTC2 | 100 | - | 566 | 590 | 578 | - | - | 0.04 | - | - | - | - | - | - | - |
| **site T6** | 120 | - | 674 | - | - | - | - | - | - | - | - | - | - | - | - |
| GTC2 | | | | | | 28.0 | 0.09 | 0.06 | | | | | 52.6 | 0.11 | 0.08 |
| av. 28 and 91 d | | | | | | 40.3 | 0.10 | 0.07 | | | | | | | |
| GTC3+GTC2 | | | | | | **28.9** | **0.08** | **0.07** | | | | | **49.8** | **0.10** | **0.09** |
| av. 28 and 91 d | | | | | | **39.4** | **0.09** | **0.08** | | | | | | | |

**Table 11.** Stabilization test results for the binders CEM III/A (a) and CEM III/B (b), and COV values for the results of three parallel compression tests. Values for $\hat{s}_x$/avg (Equation 5) were based on the results of two and three parallel tests. Curing time: 28 d and 91 d.

| **a)** | | Curing time 28 d | | | | | | | Curing time 91 d | | | | | | |
|---|---|---|---|---|---|---|---|---|---|---|---|---|---|---|---|
| Binder | Dosage | Compression | | | avg | STD | COV | $s_x$ /avg | Compression | | | avg | STD | COV | $s_x$ /avg |
| Site | (kg/m$^3$) | strength (kPa) | | | (kPa) | (kPa) | ( - ) | ( - ) | strength (kPa) | | | (kPa) | (kPa) | ( - ) | ( - ) |
| CEM | 120 | 765 | 743 | 797 | 768 | 27.2 | 0.04 | 0.04 | 1230 | 1290 | 1280 | 1267 | 26.2 | 0.02 | 0.02 |
| III/A | 150 | 1340 | 1360 | 1270 | 1323 | 47.3 | 0.04 | 0.03 | 2200 | 2190 | 2190 | 2193 | 4.7 | 0.00 | 0.00 |
| **site T1** | 100 | 538 | 499 | 498 | 512 | 22.8 | 0.04 | 0.04 | 907 | 851 | 820 | 859 | 36.0 | 0.04 | 0.05 |
| | 120 | 729 | 640 | 662 | 677 | 46.4 | 0.07 | 0.07 | 1170 | 1110 | 1230 | 1170 | 49.0 | 0.04 | 0.05 |
| | 150 | 1070 | 1030 | 1050 | 1050 | 20.0 | 0.02 | 0.02 | 1720 | 1680 | 1660 | 1687 | 24.9 | 0.01 | 0.02 |
| | 200 | 1490 | 1620 | 1580 | 1563 | 66.6 | 0.04 | 0.04 | 2610 | 2530 | 2730 | 2623 | 82.2 | 0.03 | 0.04 |
| | 120 | 682 | 607 | 688 | 659 | 45.1 | 0.07 | 0.06 | 1080 | 1150 | 1090 | 1107 | 30.9 | 0.03 | 0.03 |
| | 150 | 1100 | 1070 | - | 1085 | - | - | 0.02 | 1900 | 1850 | 1780 | 1843 | 49.2 | 0.03 | 0.03 |
| | 100 | 771 | 806 | 777 | 785 | 18.7 | 0.02 | 0.02 | 1110 | 1180 | 1180 | 1157 | 33.0 | 0.03 | 0.03 |
| | 120 | 1100 | 1160 | 1100 | 1120 | 34.6 | 0.03 | 0.03 | 1460 | 1840 | 1860 | 1720 | 184.0 | 0.11 | 0.12 |
| | 120 | 1190 | 1210 | - | 1200 | - | - | 0.01 | 1710 | 1740 | - | 1725 | - | - | 0.02 |
| | 160 | 1610 | 1570 | - | 1590 | - | - | 0.02 | 2430 | 2400 | - | 2415 | - | - | 0.01 |
| | 80 | 869 | 851 | 903 | 874 | 26.4 | 0.03 | 0.03 | 1320 | 1320 | 1400 | 1347 | 37.7 | 0.03 | 0.03 |
| | 120 | 1690 | 1730 | 1690 | 1703 | 23.1 | 0.01 | 0.01 | 2530 | 2800 | 2810 | 2713 | 129.7 | 0.05 | 0.05 |
| CEMIII/A | | | | | | 34.4 | 0.04 | 0.03 | | | | | 57.3 | 0.03 | 0.04 |
| av. 28 and 91 d | | | | | | 45.8 | 0.04 | 0.03 | | | | | | | |
| **b)** | | | | | | | | | | | | | | | |
| CEM | 120 | 546 | 538 | 546 | 543 | 4.6 | 0.01 | 0.01 | 748 | 699 | 710 | 719 | 21.0 | 0.03 | 0.03 |
| III/B | 150 | 845 | 752 | 769 | 789 | 49.5 | 0.06 | 0.06 | 1300 | 1290 | 1220 | 1270 | 35.6 | 0.03 | 0.03 |
| **site T1** | 100 | 291 | 274 | 302 | 289 | 14.1 | 0.05 | 0.05 | 424 | 402 | 416 | 414 | 9.1 | 0.02 | 0.03 |
| | 120 | 504 | 460 | 471 | 478 | 22.9 | 0.05 | 0.05 | 664 | 708 | 641 | 671 | 27.8 | 0.04 | 0.05 |
| | 150 | 807 | 772 | 786 | 788 | 17.6 | 0.02 | 0.02 | 1550 | 1450 | 1500 | 1500 | 40.8 | 0.03 | 0.03 |
| | 200 | 1360 | 1410 | 1410 | 1393 | 28.9 | 0.02 | 0.02 | 2580 | 2570 | 2680 | 2610 | 49.7 | 0.02 | 0.02 |
| | 120 | 474 | 513 | 475 | 487 | 22.2 | 0.05 | 0.04 | 880 | 814 | 956 | 883 | 58.0 | 0.07 | 0.08 |
| | 150 | 805 | 812 | 820 | 812 | 7.5 | 0.01 | 0.01 | 1520 | 1520 | 1450 | 1497 | 33.0 | 0.02 | 0.02 |
| | 100 | 470 | 456 | 453 | 460 | 9.1 | 0.02 | 0.02 | 927 | 899 | 872 | 899 | 22.5 | 0.02 | 0.03 |
| | 120 | 740 | 713 | 626 | 693 | 59.6 | 0.09 | 0.08 | 1370 | 1420 | 1230 | 1340 | 80.4 | 0.06 | 0.07 |
| | 120 | 853 | 896 | - | 875 | - | - | 0.04 | 1650 | 1620 | - | 1635 | - | - | 0.02 |
| | 160 | 1860 | 1750 | - | 1805 | - | - | 0.05 | 2870 | 3050 | - | 2960 | - | - | 0.05 |
| | 80 | 446 | 441 | 398 | 428 | 26.4 | 0.06 | 0.06 | 683 | 787 | 870 | 780 | 76.5 | 0.10 | 0.12 |
| | 120 | 1200 | 1130 | 1170 | 1167 | 35.1 | 0.03 | 0.03 | 1980 | 2140 | 2080 | 2067 | 66.0 | 0.03 | 0.04 |
| CEMIII/A | | | | | | 24.8 | 0.04 | 0.04 | | | | | 74.3 | 0.04 | 0.05 |
| av. 28 and 91 d | | | | | | 49.5 | 0.04 | 0.04 | | | | | | | |
| CEMIII/A + CEMIII/B | | | | | | **29.6** | **0.04** | **0.04** | | | | | **65.8** | **0.04** | **0.04** |
| av. 28 and 91 d | | | | | | **47.7** | **0.04** | **0.04** | | | | | | | |

**Table 12.** Stabilization test results for the binders FA+CEM II (JAM+CEM II (a), KAI+CEM II (b), and KAU+CEM II (c)) and COV values for the results of three parallel compression tests. Values for $\hat{s}_x$/avg (Equation 5) were based on the results of two and three parallel tests. Curing time: 28 d and 91 d.

| **a)** | | Curing time 28 d | | | | | | | Curing time 91 d | | | | | | |
|---|---|---|---|---|---|---|---|---|---|---|---|---|---|---|---|
| Binder | Dosage | Compression | | | avg | STD | COV | $s_x$ /avg | Compression | | | avg | STD | COV | $s_x$ /avg |
| Site | (kg/m$^3$) | strength (kPa) | | | (kPa) | (kPa) | ( - ) | ( - ) | strength (kPa) | | | (kPa) | (kPa) | ( - ) | ( - ) |
| FA | 120 | 83 | 84 | 83 | 84 | 0.7 | 0.01 | 0.01 | 105 | 108 | 102 | 105 | 2.1 | 0.02 | 0.02 |
| JAM+ | 150 | 111 | 100 | 106 | 106 | 5.8 | 0.05 | 0.06 | 140 | 138 | 133 | 137 | 2.8 | 0.02 | 0.02 |
| CEMII | 100 | 81 | 90 | 84 | 85 | 4.5 | 0.05 | 0.05 | 116 | 119 | 120 | 119 | 1.6 | 0.01 | 0.02 |
| 7:3 | 120 | 108 | 113 | 110 | 110 | 2.6 | 0.02 | 0.02 | 147 | 161 | 151 | 153 | 5.9 | 0.04 | 0.05 |
| **site T1** | 150 | 87 | 84 | 88 | 87 | 2.0 | 0.02 | 0.02 | 125 | 133 | 129 | 129 | 3.1 | 0.02 | 0.03 |
| | 200 | 159 | 156 | 156 | 157 | 1.5 | 0.01 | 0.01 | 227 | 233 | 230 | 230 | 2.6 | 0.01 | 0.01 |
| | 120 | 50 | 50 | 47 | 49 | 1.5 | 0.03 | 0.03 | 56 | 61 | 58 | 58 | 2.2 | 0.04 | 0.04 |
| | 150 | 73 | 74 | 73 | 73 | 0.7 | 0.01 | 0.01 | 102 | 88 | 87 | 93 | 7.0 | 0.08 | 0.08 |
| | 100 | 96 | 85 | 99 | 93 | 7.4 | 0.08 | 0.08 | 114 | 119 | 135 | 123 | 9.0 | 0.07 | 0.09 |
| | 120 | 144 | 124 | 125 | 131 | 11.3 | 0.09 | 0.08 | 142 | 167 | 151 | 153 | 10.3 | 0.07 | 0.08 |
| | 120 | 84 | 88 | 90 | 87 | 2.7 | 0.03 | 0.03 | 105 | 109 | 109 | 108 | 1.8 | 0.02 | 0.02 |
| | 160 | 102 | 100 | 99 | 100 | 2.0 | 0.02 | 0.02 | 140 | 133 | 132 | 135 | 3.4 | 0.02 | 0.03 |
| | 80 | 101 | 105 | 102 | 103 | 2.0 | 0.02 | 0.02 | 175 | 156 | 151 | 161 | 10.5 | 0.07 | 0.08 |
| | 120 | 236 | 236 | 227 | 233 | 5.2 | 0.02 | 0.02 | 320 | 333 | 346 | 333 | 10.5 | 0.03 | 0.04 |
| FA | 80 | 134 | 129 | 133 | 132 | 2.6 | 0.02 | 0.02 | 178 | 188 | 199 | 188 | 8.6 | 0.05 | 0.06 |
| JAM+ | 160 | 186 | 203 | 182 | 190 | 11.2 | 0.06 | 0.06 | 234 | 213 | 243 | 230 | 12.6 | 0.05 | 0.07 |
| CEMII | 120 | 104 | 80 | 78 | 87 | 14.5 | 0.17 | 0.15 | - | - | - | - | - | - | - |
| 7:3 | 160 | 129 | 129 | 114 | 124 | 8.7 | 0.07 | 0.06 | - | - | - | - | - | - | - |
| **site T4** | 120 | 56 | 78 | 67 | 67 | 11.0 | 0.16 | 0.17 | - | - | - | - | - | - | - |
| | 160 | 96 | 102 | 84 | 94 | 9.2 | 0.10 | 0.10 | - | - | - | - | - | - | - |
| FA | 120 | - | 134 | 133 | 134 | - | - | 0.01 | 199 | - | - | - | - | - | - |
| JAM+ | 120 | - | 228 | 220 | 224 | - | - | 0.03 | 381 | - | - | - | - | - | - |
| CEMII | 160 | - | 241 | 237 | 239 | - | - | 0.01 | 339 | - | - | - | - | - | - |
| 7:3 | 120 | - | 336 | 328 | 332 | - | - | 0.02 | 412 | - | - | - | - | - | - |
| **site T3** | 120 | - | 338 | 341 | 340 | - | - | 0.01 | 433 | - | - | - | - | - | - |
| | 150 | - | 489 | 486 | 488 | - | - | 0.01 | 670 | - | - | - | - | - | - |
| FA JAM+CEMII 7/3 | | | | | | 5.3 | 0.05 | 0.04 | | | | | 5.9 | 0.04 | 0.05 |
| av. 28 and 91 d | | | | | | 5.6 | 0.05 | 0.04 | | | | | | | |
| **b)** | | | | | | | | | | | | | | | |
| FA | 80 | 82 | 85 | - | 84 | - | - | 0.03 | 129 | - | - | - | - | - | - |
| KAI+ | 80 | 43 | 45 | - | 44 | - | - | 0.06 | 63 | - | - | - | - | - | - |
| CEMII | 120 | 209 | 232 | - | 221 | - | - | 0.09 | 333 | - | - | - | - | - | - |
| 7:3 | 120 | 138 | 119 | - | 129 | - | - | 0.13 | 203 | - | - | - | - | - | - |
| **site T3** | 120 | 323 | 320 | - | 322 | - | - | 0.01 | 489 | - | - | - | - | - | - |
| | 160 | - | 330 | - | - | - | - | - | 415 | - | - | - | - | - | - |

*Continued on next page*

| **b)** | | Curing time 28 d | | | | | | | Curing time 91 d | | | | | | |
|---|---|---|---|---|---|---|---|---|---|---|---|---|---|---|---|
| Binder | Dosage | Compression | | | avg | STD | COV | $s_x$ /avg | Compression | | | avg | STD | COV | $s_x$ /avg |
| Site | (kg/m$^3$) | strength (kPa) | | | (kPa) | (kPa) | ( - ) | ( - ) | strength (kPa) | | | (kPa) | (kPa) | ( - ) | ( - ) |
| | 160 | 258 | 286 | - | 272 | - | - | 0.09 | 341 | - | - | - | - | - | - |
| | 80 | 195 | 174 | - | 185 | - | - | 0.10 | 274 | - | - | - | - | - | - |
| | 80 | 129 | 124 | - | 127 | - | - | 0.04 | 205 | - | - | - | - | - | - |
| | 120 | 319 | 313 | - | 316 | - | - | 0.02 | 472 | - | - | - | - | - | - |
| | 120 | 216 | 207 | - | 212 | - | - | 0.04 | 326 | - | - | - | - | - | - |
| | 120 | 306 | 314 | - | 310 | - | - | 0.02 | 442 | - | - | - | - | - | - |
| | 150 | 470 | 468 | - | 469 | - | - | 0.00 | 647 | - | - | - | - | - | - |
| | 150 | 334 | 343 | - | 339 | - | - | 0.02 | 458 | - | - | - | - | - | - |
| | 160 | 470 | 468 | - | 469 | - | - | 0.00 | 647 | - | - | - | - | - | - |
| | 160 | 334 | 343 | - | 339 | - | - | 0.02 | 458 | - | - | - | - | - | - |
| FA KAI+CEMII 7/3 | | | | | | - | - | 0.05 | | | | | - | - | - |
| av. 28 and 91 d | | | | | | - | - | - | | | | | | | - |
| **c)** | | | | | | | | | | | | | | | |
| FA | 120 | 91 | 84 | 95 | 90 | 5.2 | 0.06 | 0.06 | 142 | 147 | 147 | 145 | 2.4 | 0.02 | 0.02 |
| KAU+ | 150 | 223 | 237 | 233 | 231 | 7.3 | 0.03 | 0.03 | 210 | 212 | 211 | 211 | 1.0 | 0.00 | 0.01 |
| CEMII | 100 | 99 | 100 | 93 | 97 | 3.4 | 0.03 | 0.03 | 129 | 128 | 133 | 130 | 2.2 | 0.02 | 0.02 |
| 7:3 | 120 | 128 | 137 | 131 | 132 | 4.6 | 0.04 | 0.03 | 189 | 183 | 179 | 184 | 4.2 | 0.02 | 0.03 |
| **site T1** | 150 | 154 | 151 | 157 | 154 | 3.2 | 0.02 | 0.02 | 195 | 186 | 192 | 191 | 3.8 | 0.02 | 0.02 |
| | 200 | 278 | 292 | 261 | 277 | 15.4 | 0.06 | 0.06 | 383 | 375 | 379 | 379 | 3.1 | 0.01 | 0.01 |
| | 120 | 91 | 96 | 95 | 94 | 2.7 | 0.03 | 0.03 | 116 | 116 | 108 | 113 | 4.2 | 0.04 | 0.04 |
| | 150 | 161 | 151 | 165 | 159 | 7.3 | 0.05 | 0.05 | 186 | 177 | 187 | 183 | 4.6 | 0.02 | 0.03 |
| | 100 | 102 | 110 | 111 | 108 | 4.9 | 0.05 | 0.04 | 130 | 133 | 125 | 129 | 3.3 | 0.03 | 0.03 |
| | 120 | 148 | 157 | 145 | 150 | 6.2 | 0.04 | 0.04 | 179 | 180 | 180 | 180 | 0.5 | 0.00 | 0.00 |
| | 120 | 102 | 101 | 104 | 102 | 1.3 | 0.01 | 0.01 | 137 | 137 | 129 | 134 | 3.6 | 0.03 | 0.03 |
| | 160 | 155 | 152 | 159 | 155 | 3.2 | 0.02 | 0.02 | 196 | 195 | 195 | 195 | 0.6 | 0.00 | 0.00 |
| | 80 | 115 | 92 | 120 | 109 | 15.0 | 0.14 | 0.13 | 170 | 173 | 170 | 171 | 1.2 | 0.01 | 0.01 |
| | 120 | 252 | 247 | 242 | 247 | 5.1 | 0.02 | 0.02 | 431 | 424 | 413 | 423 | 7.3 | 0.02 | 0.02 |
| FA | 120 | 216 | 196 | 209 | 207 | 10.3 | 0.05 | 0.05 | 283 | 285 | 302 | 290 | 8.5 | 0.03 | 0.03 |
| KAU+ | 160 | 349 | 393 | 403 | 382 | 28.5 | 0.07 | 0.07 | 536 | 554 | 554 | 548 | 8.4 | 0.02 | 0.02 |
| CEMII | 120 | 225 | 216 | 233 | 225 | 8.3 | 0.04 | 0.04 | - | - | - | - | - | - | - |
| 7:3 | 120 | 116 | 84 | 110 | 104 | 16.9 | 0.16 | 0.16 | 157 | 164 | 159 | 160 | 2.8 | 0.02 | 0.02 |
| **site T4** | 160 | 216 | 206 | 230 | 218 | 12.2 | 0.06 | 0.06 | 289 | 269 | 298 | 285 | 12.3 | 0.04 | 0.05 |
| FA KAU+CEMII 7/3 | | | | | | 8.5 | 0.05 | 0.05 | | | | | 4.1 | 0.02 | 0.02 |
| av. 28 and 91 d | | | | | | 6.3 | 0.03 | 0.04 | | | | | | | |
| FA JAM / KAI / KAU + CEMII 7/3 | | | | | | **6.9** | **0.05** | **0.05** | | | | | **5.0** | **0.03** | **0.03** |
| | | | | | | **5.9** | **0.04** | **0.04** | | | | | | | |

**Table 13.** Stabilization test results for the binders Stabi65 and Stabi80, and COV values for the results of three parallel compression tests. Values for $\hat{s}_x$/avg (Equation 5) were based on the results of two and three parallel tests. Curing time: 28 d and 91 d.

| | | Curing time 28 d | | | | | | | Curing time 91 d | | | | | | |
|---|---|---|---|---|---|---|---|---|---|---|---|---|---|---|---|
| Binder | Dosage | Compression | | | avg | STD | COV | $s_x$ /avg | Compression | | | avg | STD | COV | $s_x$ /avg |
| Site | (kg/m$^3$) | strength (kPa) | | | (kPa) | (kPa) | ( - ) | ( - ) | strength (kPa) | | | (kPa) | (kPa) | ( - ) | ( - ) |
| Stabi65 | 100 | 412 | - | - | - | - | - | - | - | - | - | - | - | - | - |
| **site T6** | 120 | 731 | 661 | - | 696 | - | - | 0.09 | - | - | - | - | - | - | - |
| | 140 | 880 | 841 | - | 861 | - | - | 0.04 | - | - | - | - | - | - | - |
| | 160 | 1280 | 1130 | - | 1205 | - | - | 0.11 | - | - | - | - | - | - | - |
| Stabi80 | 80 | 231 | 218 | - | 225 | - | - | 0.05 | 344 | 331 | - | 338 | - | - | 0.03 |
| **site T3** | 120 | 487 | 439 | - | 463 | - | - | 0.09 | 613 | 625 | - | 619 | - | - | 0.02 |
| | 80 | 447 | 447 | - | 447 | - | - | 0.00 | 613 | 579 | - | 596 | - | - | 0.05 |
| | 120 | 708 | 731 | - | 720 | - | - | 0.03 | 1070 | 1040 | - | 1055 | - | - | 0.03 |
| Stabi80 | 135 | 302 | 306 | - | 304 | - | - | 0.01 | 412 | 400 | - | 406 | - | - | 0.03 |
| **site T5** | 100 | 255 | 254 | - | 255 | - | - | 0.00 | 324 | - | - | - | - | - | - |
| | 135 | 381 | 398 | - | 390 | - | - | 0.04 | 509 | - | - | - | - | - | - |
| | 170 | 375 | 445 | - | 410 | - | - | 0.15 | 634 | - | - | - | - | - | - |
| | 100 | 281 | 275 | - | 278 | - | - | 0.02 | 376 | 386 | - | 381 | - | - | 0.02 |
| | 135 | 529 | 508 | - | 519 | - | - | 0.04 | 756 | 749 | - | 753 | - | - | 0.01 |
| | 170 | 375 | 445 | - | 410 | - | - | 0.15 | 634 | - | - | - | - | - | - |
| | 100 | 264 | 268 | - | 266 | - | - | 0.01 | 290 | - | - | - | - | - | - |
| | 135 | 447 | 445 | - | 446 | - | - | 0.00 | 517 | - | - | - | - | - | - |
| | 170 | 592 | 595 | - | 594 | - | - | 0.00 | 753 | - | - | - | - | - | - |
| | 100 | 308 | 285 | - | 297 | - | - | 0.07 | 407 | 377 | - | 392 | - | - | 0.07 |
| | 135 | 418 | 471 | - | 445 | - | - | 0.11 | 710 | 657 | - | 684 | - | - | 0.07 |
| | 135 | 456 | 475 | - | 466 | - | - | 0.04 | 564 | 586 | - | 575 | - | - | 0.03 |
| | 135 | 218 | 230 | - | 224 | - | - | 0.05 | 386 | 342 | - | 364 | - | - | 0.11 |
| Stabi80 | 70 | 278 | 281 | - | 280 | - | - | 0.01 | 382 | 368 | - | 375 | - | - | 0.03 |
| **site T2** | 110 | 579 | - | - | - | - | - | - | 607 | 684 | - | 646 | - | - | 0.11 |
| | 150 | 630 | 474 | 453 | 519 | 96.7 | 0.19 | 0.17 | 611 | 505 | - | 558 | - | - | 0.17 |
| | 70 | 232 | 230 | - | 231 | - | - | 0.01 | 314 | 295 | - | 305 | - | - | 0.06 |
| | 110 | 379 | - | - | - | - | - | - | 553 | 505 | - | 529 | - | - | 0.08 |
| | 150 | 661 | 708 | - | 685 | - | - | 0.06 | 918 | 1080 | - | 999 | - | - | 0.14 |
| | 70 | 308 | 279 | - | 294 | - | - | 0.09 | 427 | 407 | - | 417 | - | - | 0.04 |
| | 110 | 513 | 471 | - | 492 | - | - | 0.08 | 876 | 790 | - | 833 | - | - | 0.09 |
| | 150 | 1040 | 1050 | - | 1045 | - | - | 0.01 | - | - | - | - | - | - | - |
| Stabi80 | 80 | 97 | 102 | 102 | 100 | 2.4 | 0.02 | 0.03 | 128 | 122 | 125 | 125 | 2.4 | 0.02 | 0.02 |
| **site T4** | 120 | 161 | 129 | 128 | 139 | 15.3 | 0.11 | 0.12 | 182 | 194 | 177 | 184 | 7.1 | 0.04 | 0.05 |
| Stabi80+65 | | | | | | 38.1 | 0.11 | 0.06 | | | | | 52.6 | 0.11 | 0.06 |
| av. 28 and 91 d | | | | | | 21.5 | 0.07 | 0.06 | | | | | | | |
| FA JAM/KAI/KAU+CEMII. Stabi80+65 | | | | | | **17.3** | **0.07** | **0.05** | | | | | **4.9** | **0.03** | **0.04** |
| av. 28 and 91 d | | | | | | **11.1** | **0.05** | **0.05** | | | | | | | |

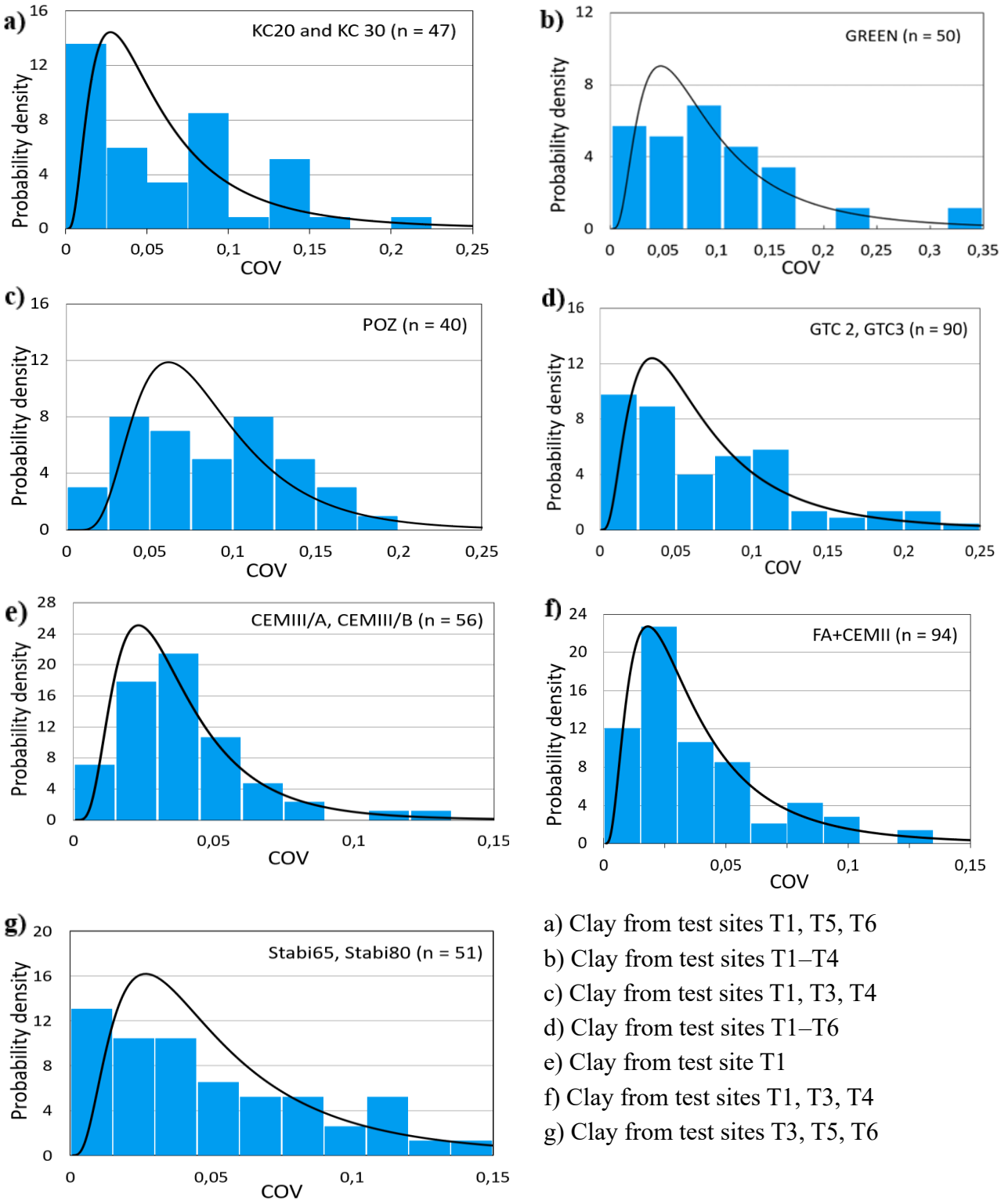


a) Clay from test sites T1, T5, T6
b) Clay from test sites T1–T4
c) Clay from test sites T1, T3, T4
d) Clay from test sites T1–T6
e) Clay from test site T1
f) Clay from test sites T1, T3, T4
g) Clay from test sites T3, T5, T6

**Figure 7.** Correlation of COV and probability density of stabilization tests with different binders. Curing time: 28 d or 91 d. (a) KC20 and KC30, (b) GREEN, (c) POZ, (d) GTC2 and GTC3, (e) CEM III/A and CEM III/B, (f) FA+CEM II (JAM+CEM II, KAI+CEM II and KAU+CEM II), and (g) Stabi65 and Stabi80.

Figures 7a-f illustrates the distribution of the COV values of the stabilization test results for a

specific binder. The distributions were observed to resemble log-normal distributions. Therefore, the corresponding log-normal distributions were fitted to the data via the method of moments.

Table 14 presents the sample statistics (mean and SD) used to fit the log-normal distributions together with the derived 5% and 95% percentiles. Most binders have percentiles in the ranges of $COV_{5\%} \approx 0.01–0.02$ and $COV_{95\%} \approx 0.1–0.2$. However, the calcareous binders GREEN and POZ have wider percentile ranges: $COV_{5\%} \approx 0.02–0.04$ and $COV_{95\%} \approx 0.2–0.3$, respectively. Meanwhile, the FA-containing binders JAM/KAI/KAU+CEM II have the narrowest percentile range ($COV_{5\%} \approx 0.01$ and $COV_{95\%} \approx 0.1$). In general, the mode value (the greatest likelihood) was found to be in the range of COV = 0.02–0.05.

**Table 14.** Stabilization test results. Sample statistics (mean and SD) for the COV values defined via $\hat{s}_x$ and the 5% and 95% percentiles were defined using the fitted log-normal distributions.

| Binder | $\mu_{COV}$ ($COV_{av.}$) | $SD_{COV}$ | $COV_{5\%}$ | $COV_{95\%}$ |
|---|---|---|---|---|
| KC20 and KC30 (calcareous) | 0.065 | 0.057 | 0.014 | 0.169 |
| GREEN (calcareous) | 0.103 | 0.085 | 0.024 | 0.259 |
| POZ (calcareous) | 0.087 | 0.045 | 0.035 | 0.173 |
| GTC2 and GTC3 (gypsum-containing) | 0.075 | 0.062 | 0.018 | 0.190 |
| CEM III/A and CEM III/B (BFS-containing) | 0.038 | 0.024 | 0.013 | 0.084 |
| JAM/KAI/KAU+CEM II (FA-containing) | 0.041 | 0.035 | 0.009 | 0.106 |
| Stabi65 and Stabi80 (FA-containing) | 0.057 | 0.047 | 0.014 | 0.144 |

### *3.3. Field to laboratory shear strength ratio pairs and results*

The resulting pairs of field strength to laboratory strength ratios and the average strength from stabilization tests were compiled into figures by binder ($k_{F/L\ pair}$; see Section 2.1 and Equation 1). Trend graphs were also formed. The number of result pairs per test site and binders used in the formation of the graphs is shown in Table 15 (the result pairs are from six test sites).

Field to laboratory shear strength ratios $k_{F/L}$ were determined and plotted as a function of laboratory strength $\tau_{lab}$ for each binder. The Figures 8–14 show the determined field to laboratory shear strength ratios and their corresponding trend graphs as follows:

- Lime cement (KC20 and KC30): Figure 8;
- GREEN: Figure 9;
- POZ: Figure 10;
- GTC (GTC2 and GTC3), Figure 11;
- CEM III (CEM III/A and CEM III/B): Figure 12;
- FA+CEM II (JAM+CEM II, KAI+CEM II, KAU+CEM II): Figure 13;

Stabi (Stabi65 and Stabi80): Figure 14.

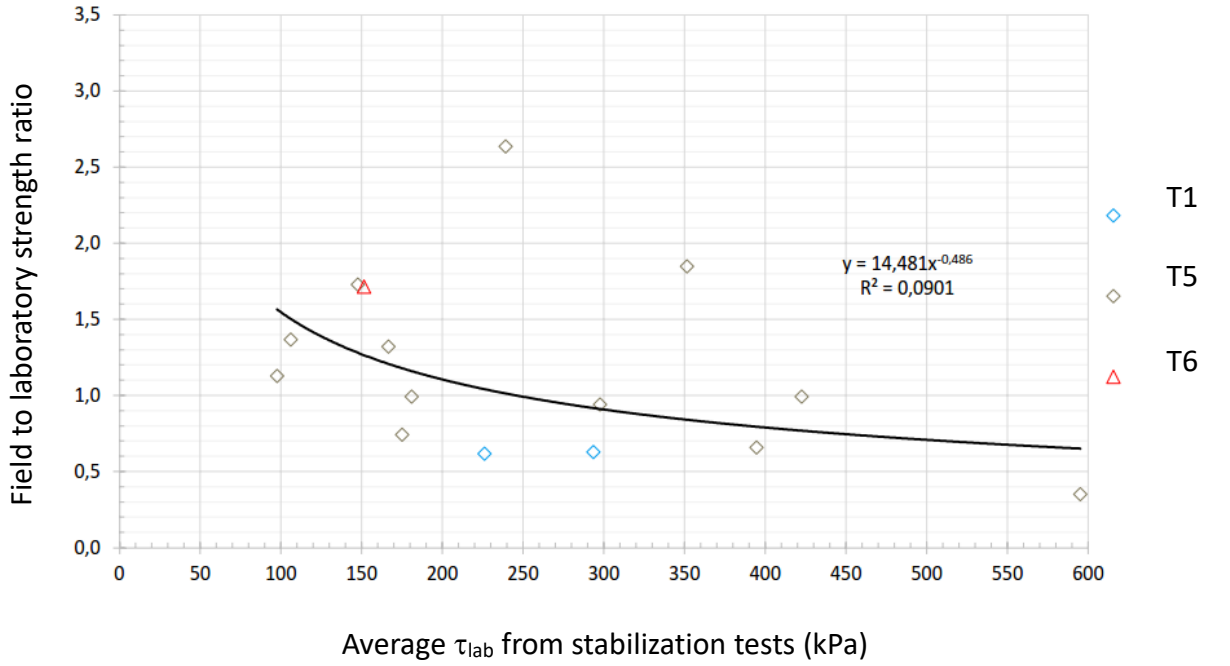


**Figure 8.** Lime cement binders (KC20 and KC30). Field to laboratory shear strength ratio and laboratory shear strength of the soil mixes. Field and laboratory shear strengths are based on QC soundings and stabilization test results (average of parallel sounding and test results).

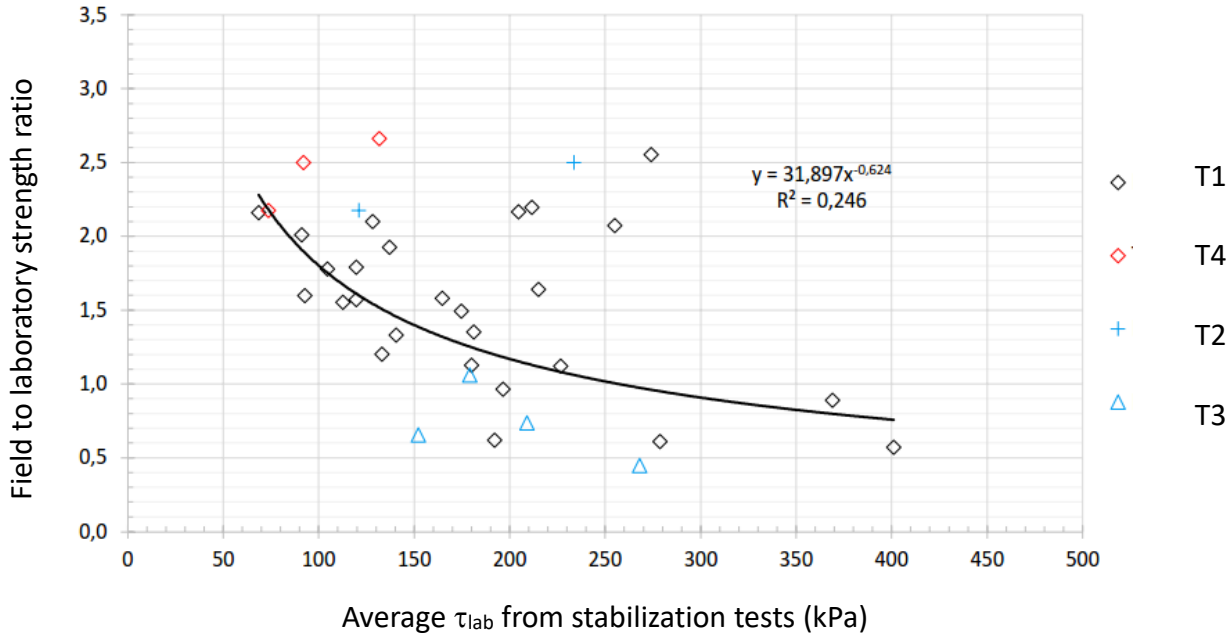


**Figure 9.** The GREEN binder. Field to laboratory shear strength ratio and laboratory shear strength of the soil mix.

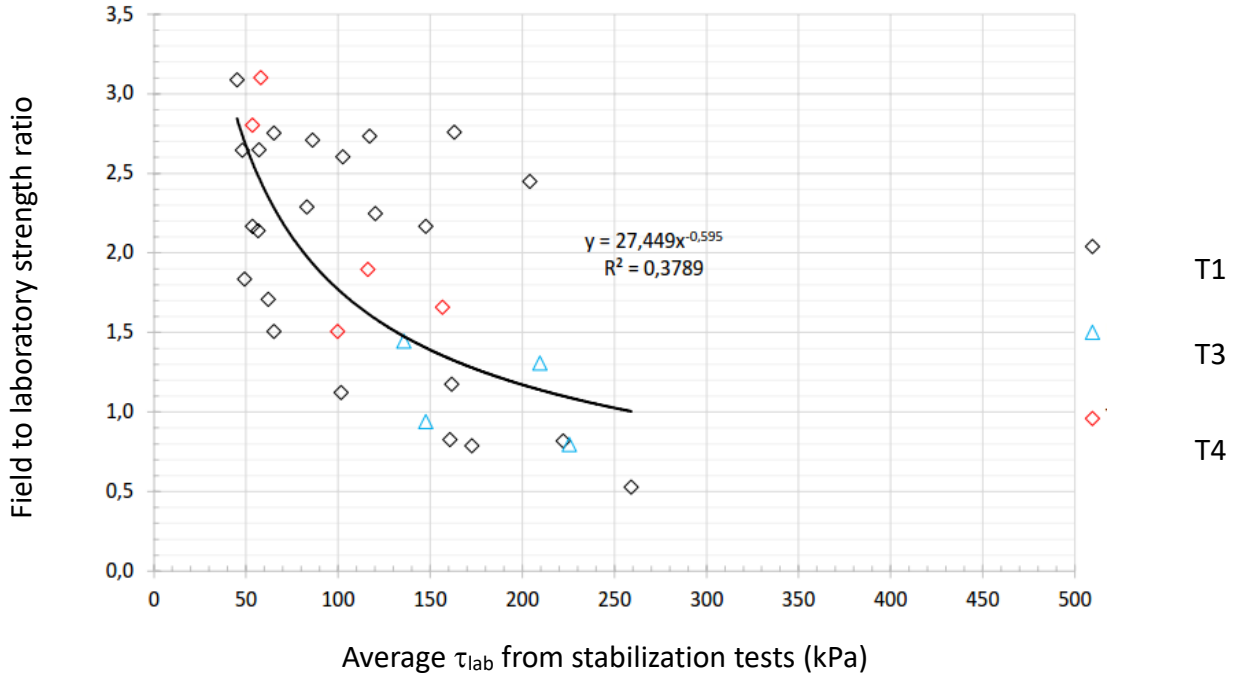


**Figure 10.** The POZ binder. Field to laboratory shear strength ratio and laboratory shear strength of the soil mix.

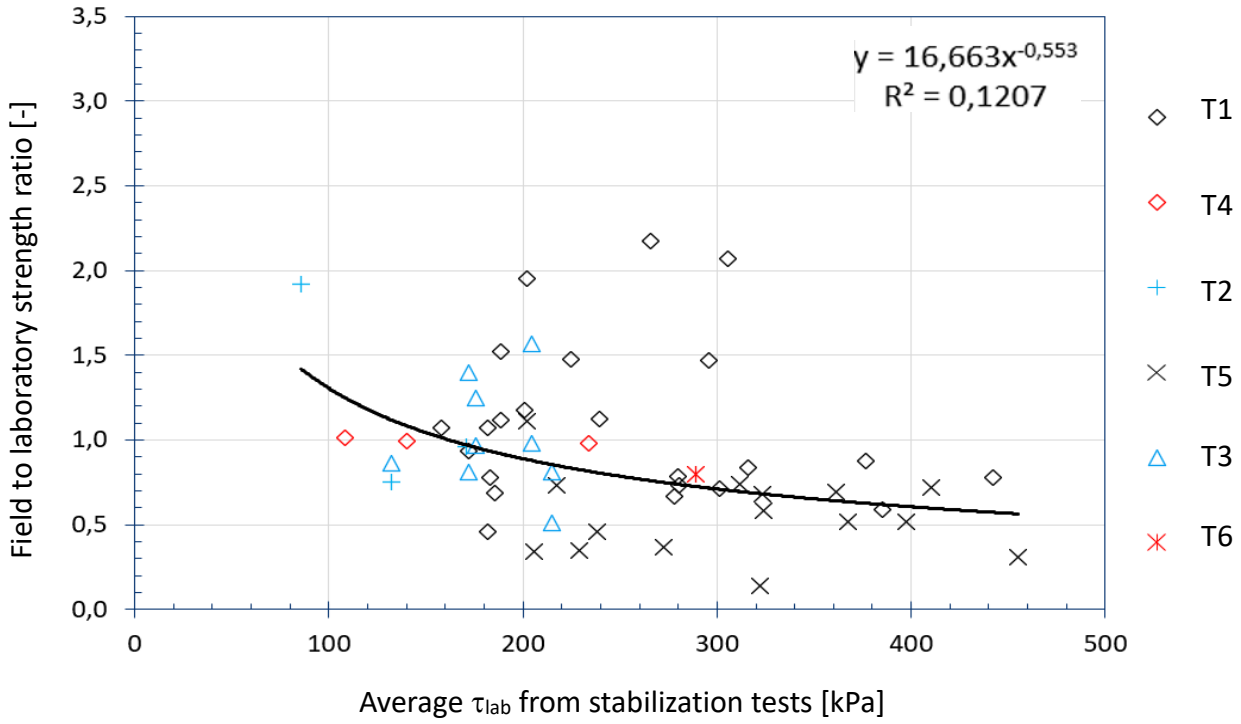


**Figure 11.** GTC binders (GTC2 and GTC3). Field to laboratory shear strength ratio and laboratory shear strength of the soil mix.

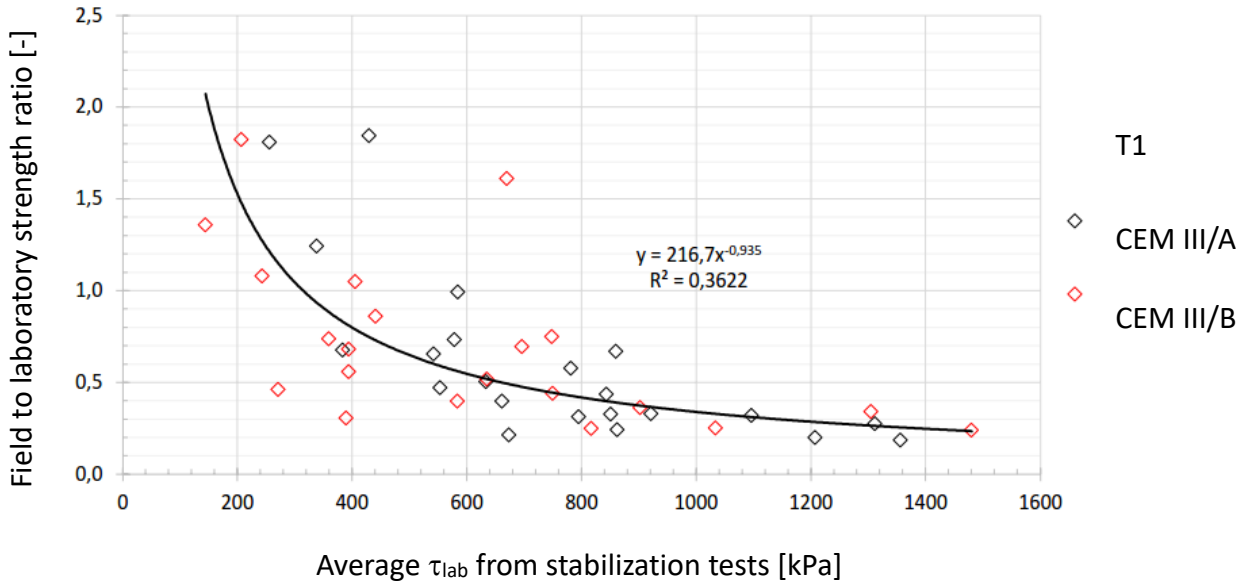


**Figure 12.** CEM III binders (CEM III/A and CEM III/B). Field to laboratory shear strength ratio and laboratory shear strength of the soil mixes.

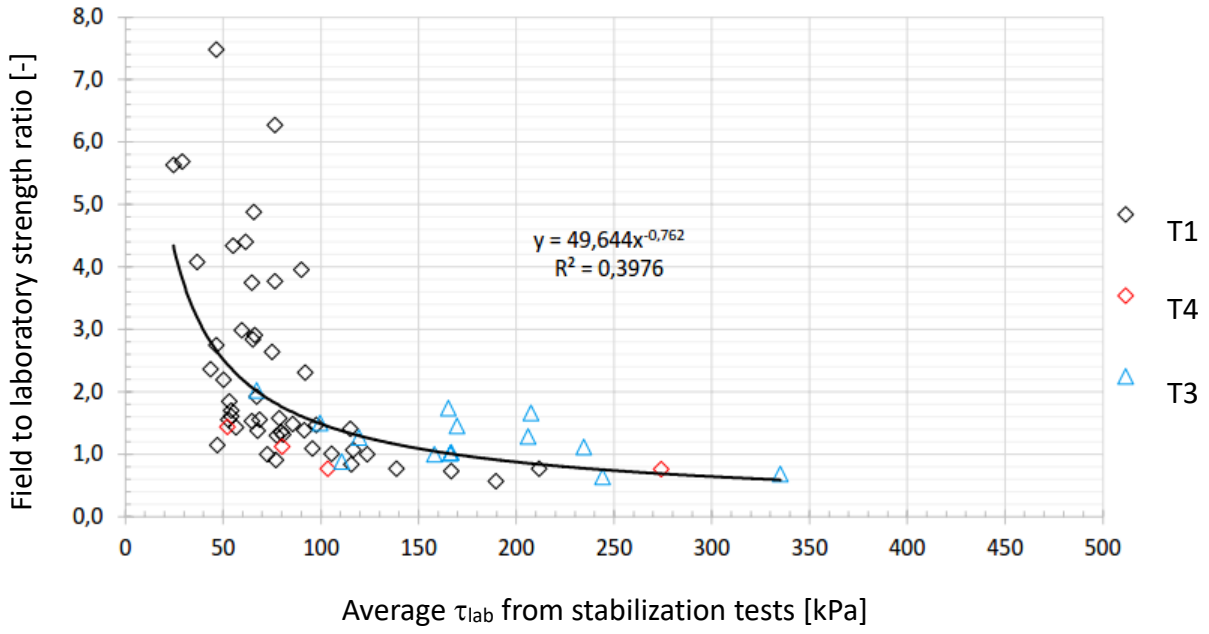


**Figure 13.** FA+CEM II binders (JAM+CEM II, KAI+CEM II, and KAU+CEM II). Field to laboratory shear strength ratio and laboratory shear strength of the soil mixes.

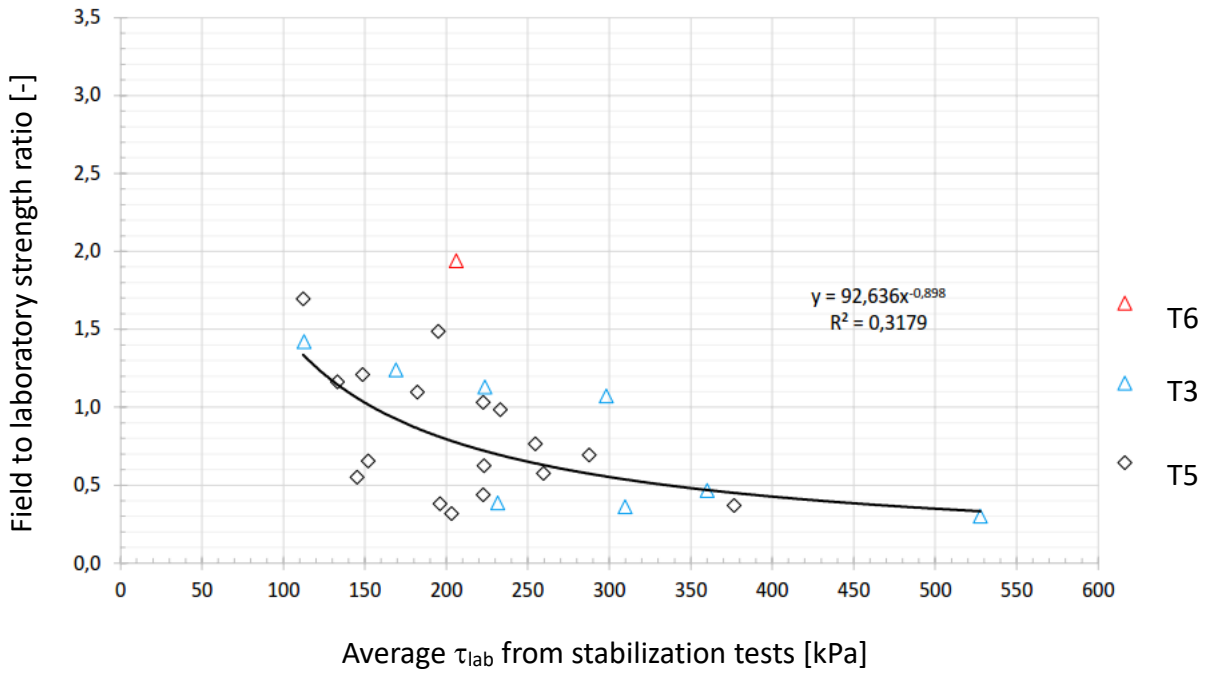


**Figure 14.** InfraStabi binders (Stabi65 and Stabi80). Field to laboratory shear strength ratio and laboratory shear strength of the soil mixes.

**Table 15.** The number of result pairs $k_{F/Lpair}$ used to determine the field to laboratory strength ratio $k_{F/L}$ nomogram.

| Binder type | Calcareous | | | Gypsum | BFS | FA-containing | | |
|---|---|---|---|---|---|---|---|---|
| Binder | KC | GREEN | POZ | GTC | CEM III | FA+CEM II | Stabi | Σ |
| Test site T1 | – | 26 | 23 | 23 | 44 | 48 | – | 164 |
| T2 | 2 | 2 | – | 3 | – | – | – | 7 |
| T3 | – | 4 | 4 | 9 | – | 14 | 8 | 39 |
| T4 | – | 3 | 5 | 3 | – | 6 | – | 17 |
| T5 | 12 | – | – | 15 | – | – | 17 | 44 |
| T6 | 1 | – | – | 1 | – | – | 1 | 3 |
| Σ | 15 | 35 | 32 | 54 | 44 | 68 | 26 | 274 |

### *3.4. Field to laboratory strength ratio: Transformation uncertainty and simulation-based validation*

The defined transformation uncertainties for each nomogram trendline by binder are collected in Table 16. All trendlines have a small bias ($b \approx 1.1$); the mean bias is often found to be slightly greater than 1 because the error terms tend to follow a log-normal distribution (see, e.g., [88]), as was observed in the residual analysis (see Figure 15b). Figure 15a also illustrates the trendline ± 1 SD scatter lines calculated via the transformation uncertainty $\delta$ (COV). Transformation uncertainties were found to be mostly in the range of $\delta = 0.4–0.5$, i.e., medium variability [89]. As a comparison, transformation models which are used to estimate geotechnical properties using indirect methods usually have $\delta = 0.3–0.9$ [90].

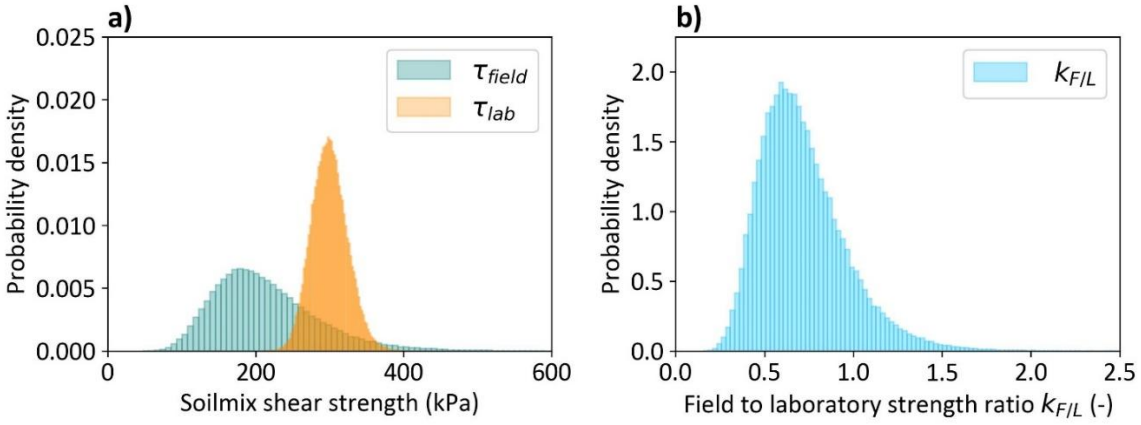


**Figure 15.** Example of probability density histograms for (a) $\tau_{lab}$ and $\tau_{field}$ values; (b) field to laboratory ratios $k_{F/L}$ for a Monte Carlo simulation (GTC binder).

**Table 16.** The transformation uncertainties in the trendlines used to define characteristic "cautious mean" curves and the results of the simulation-based validation.

| Binder type | Trendline ($x = \tau_{lab}$ in kPa) | $n$ | Bias $b$ | $\delta$ (COV) | $COV_{av}$, $\tau_{lab}$ | $COV_{av}$, $\tau_{field}$ | Validation |
|---|---|---|---|---|---|---|---|
| Calcareous binders | | | | | | | |
| Lime cement (KC20, KC30) | $k_{F/L} = 14.481x^{-0.486}$ | 15 | 1.12 | 0.532 | 0.09 | 0.36 | A |
| GREEN | $k_{F/L} = 31.897x^{-0.624}$ | 35 | 1.09 | 0.447 | 0.09 | 0.36 | C |
| POZ | $k_{F/L} = 27.449x^{-0.595}$ | 32 | 1.11 | 0.382 | 0.09 | 0.36 | C |
| Gypsum-containing binders | | | | | | | |
| GTC (GTC2, GTC3) | $k_{F/L} = 16.663x^{-0.553}$ | 54 | 1.11 | 0.476 | 0.08 | 0.33 | B |
| Blast furnace slag binders | | | | | | | |
| CEM III/A and CEM III/B | $k_{F/L} = 216.7x^{-0.935}$ | 44 | 1.12 | 0.547 | 0.04 | 0.48 | B |
| FA-containing binders | | | | | | | |
| JAM/KAI/KAU+CEM II | $k_{F/L} = 49.644x^{-0.762}$ | 68 | 1.12 | 0.530 | 0.05 | 0.33 | B |
| Stabi (Stabi65, Stabi80) | $k_{F/L} = 92.636x^{-0.898}$ | 26 | 1.10 | 0.450 | 0.05 | 0.33 | C |

Note: A, aligns well, slightly larger than the characteristic $k_{F/L}$; B, aligns well, slightly larger than the characteristic $k_{F/L}$ at smaller laboratory shear strength values; C, aligns almost entirely with the characteristic curve.

Simulation-based validation of the defined characteristic trendlines was performed using the average COV values listed in Table 16. Figures 15 and 16–22 illustrate this validation. The characteristic trendline (which would roughly correspond to a 31% percentile) was found to be mostly in good agreement with the 31% percentiles calculated using the generated $k_{F/L}$ values. The graphs illustrating the other simulation-based validations are presented in Figures 16–22. The results of the validation are collected in Table 16. For all the studied binders, the 31% percentiles calculated from simulated values

corresponded well with the characteristic "cautious" curve. The characteristic trendlines derived using Equation 7 with the determined $\delta$ values are collected in Figures 23–26.

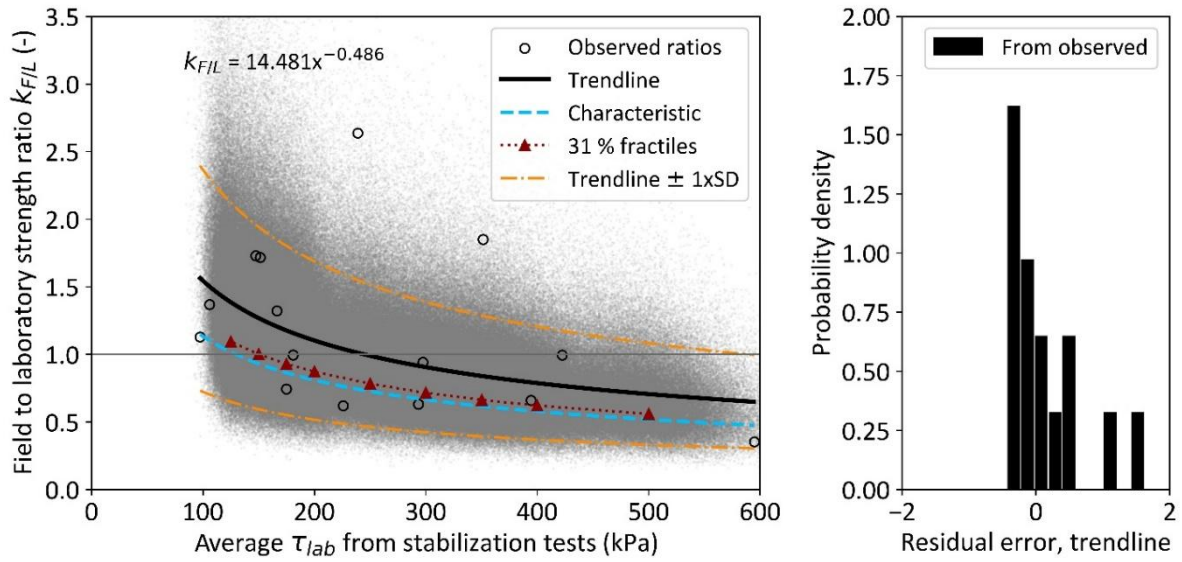


**Figure 16.** Monte Carlo simulation (KC20 and KC30): Characteristic curve, trendline with ± 1 SD lines, and 31% percentiles of simulated ratios (left) and residual analysis (right).

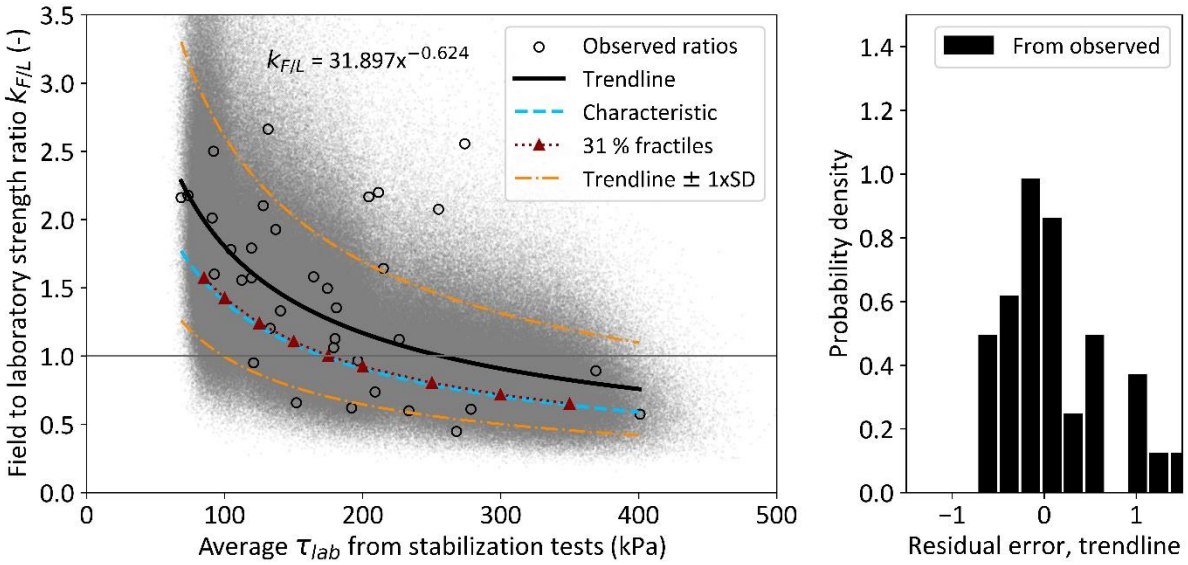


**Figure 17.** Monte Carlo simulation (GREEN): 31% characteristic curve, trendline with ± 1 SD lines, and 31% percentiles of simulated ratios (left) and residual analysis (right).

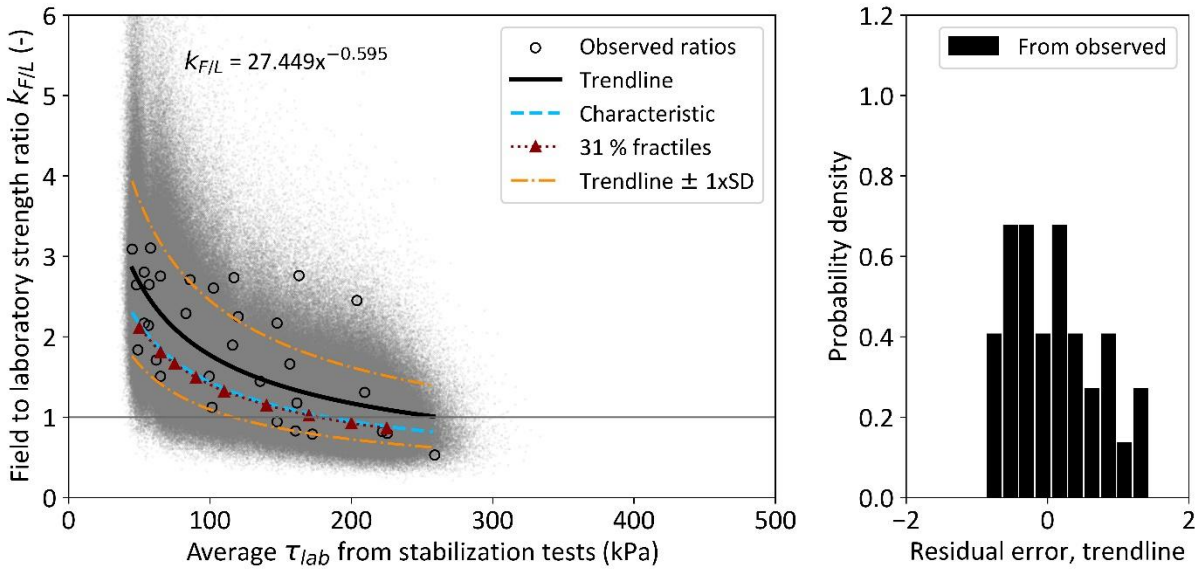


**Figure 18.** Monte Carlo simulation (POZ): characteristic curve, trendline with ± 1 SD lines, and 31% percentiles of simulated ratios (left) and residual analysis (right).

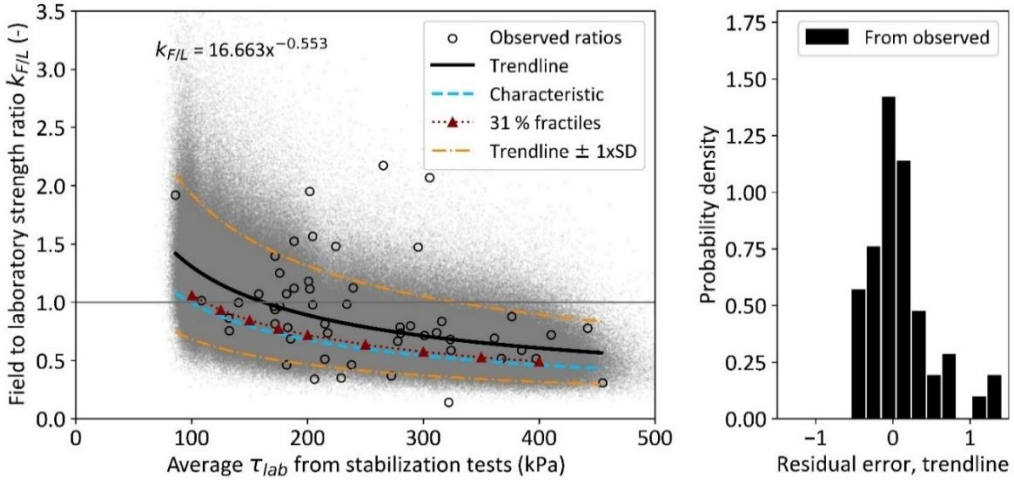


**Figure 19.** Monte Carlo simulation (GTC2 and GTC3): Characteristic curve, trendline with ± 1 SD lines and 31% percentiles of simulated ratios (left) and residual analysis (right).

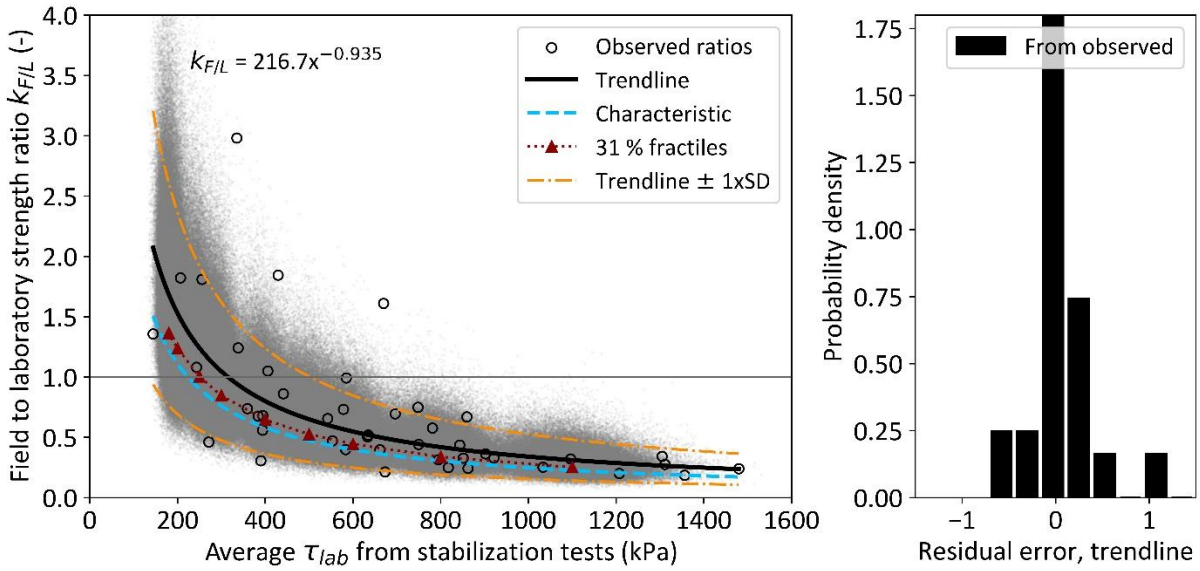


**Figure 20.** Monte Carlo simulation (CEM III/A and CEMIII/B ): Characteristic curve, trendline with ± 1 SD lines, and 31% percentiles of simulated ratios (left) and residual analysis (right).

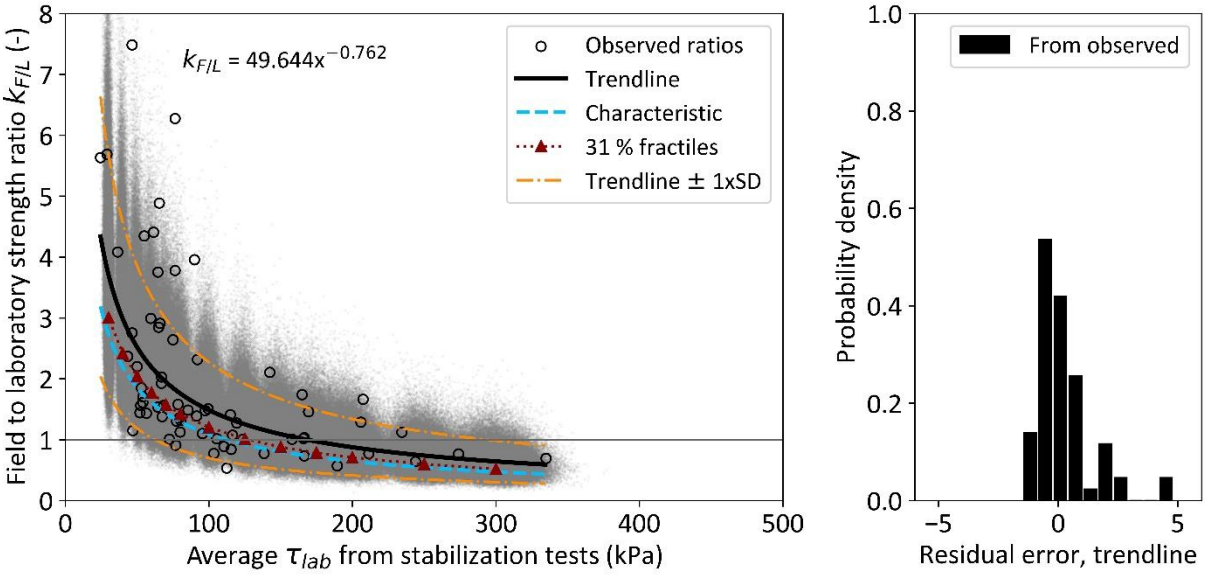


**Figure 21.** Monte Carlo simulation (FA+CEM II): Characteristic curve, trendline with ± 1 SD lines, and 31% percentiles of simulated ratios (left) and residual analysis (right).

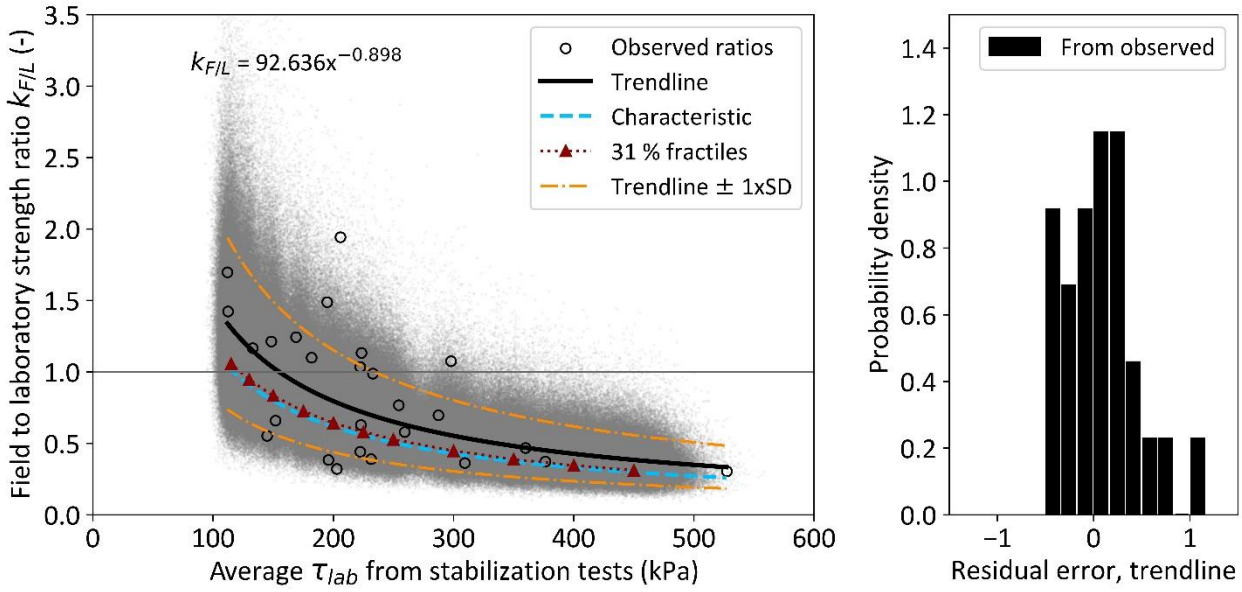


**Figure 22.** Monte Carlo simulation (Stabi65 and Stabi80): Characteristic curve, trendline with ± 1 SD lines, and 31% percentiles of simulated ratios (left) and residual analysis (right).

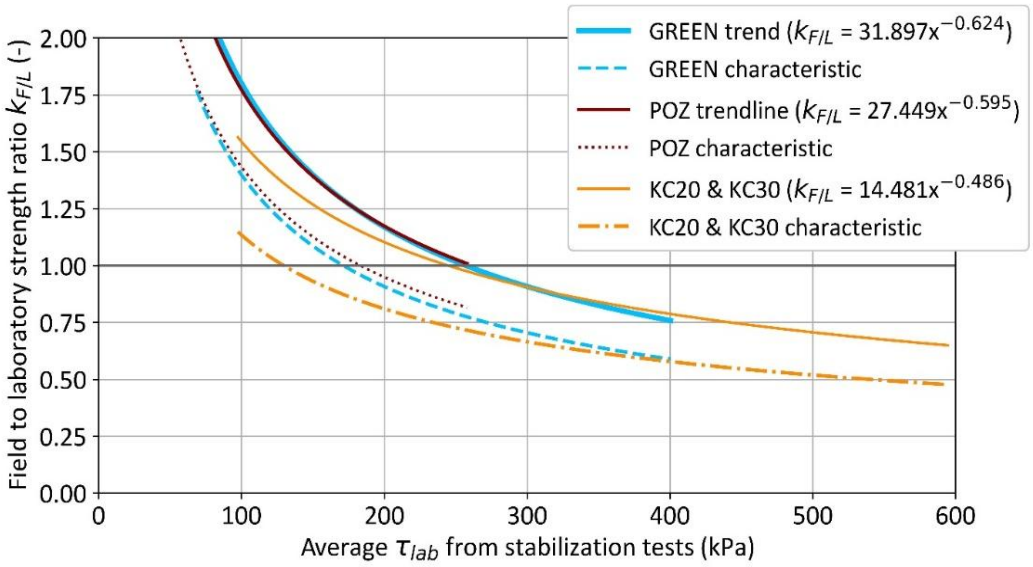


**Figure 23.** Calcareous binders (KC20, KC30, GREEN, and POZ). Trendline and the characteristic "cautious mean" curve for estimating the field to laboratory shear strength ratio from the average $\tau_{lab}$ for column-stabilized soil mixes.

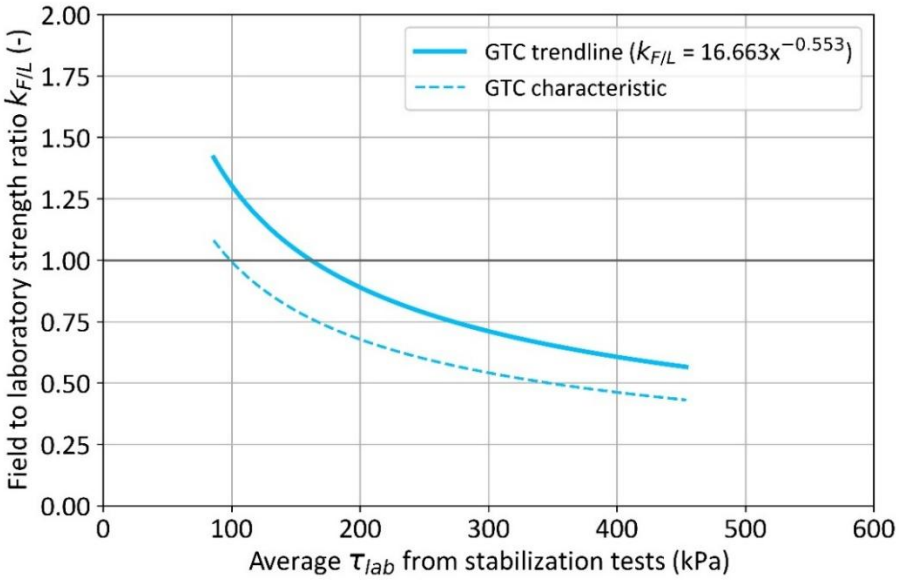


**Figure 24.** Gypsum-containing binders (GTC2 and GTC3). Trendline and the characteristic "cautious mean" curve for estimating the field to laboratory shear strength ratio from the average $\tau_{lab}$ for column-stabilized soil mixes.

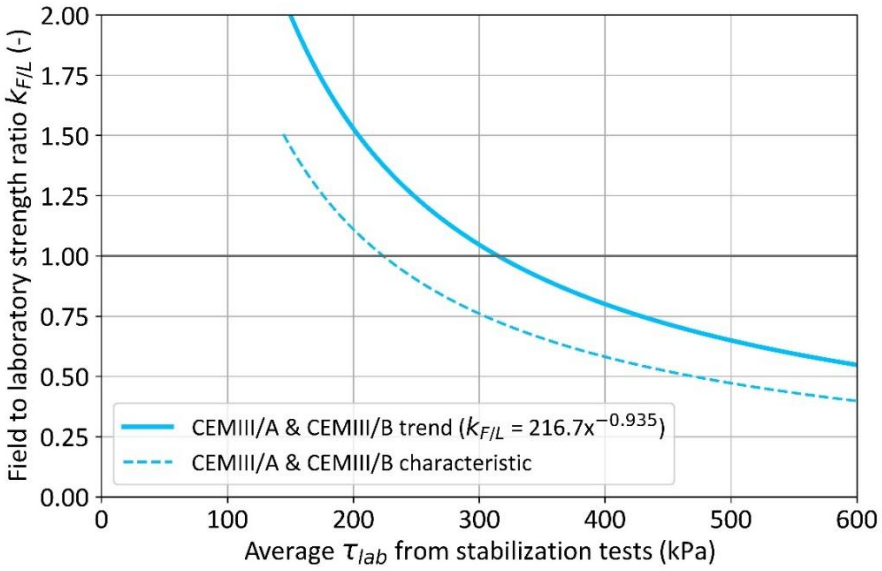


**Figure 25.** BSF-containing binders (CEM III/A and CEM III/B). Trendline and the characteristic "cautious mean" curve for estimating the field to laboratory shear strength ratio from the average $\tau_{lab}$ for column-stabilized soil mixes.

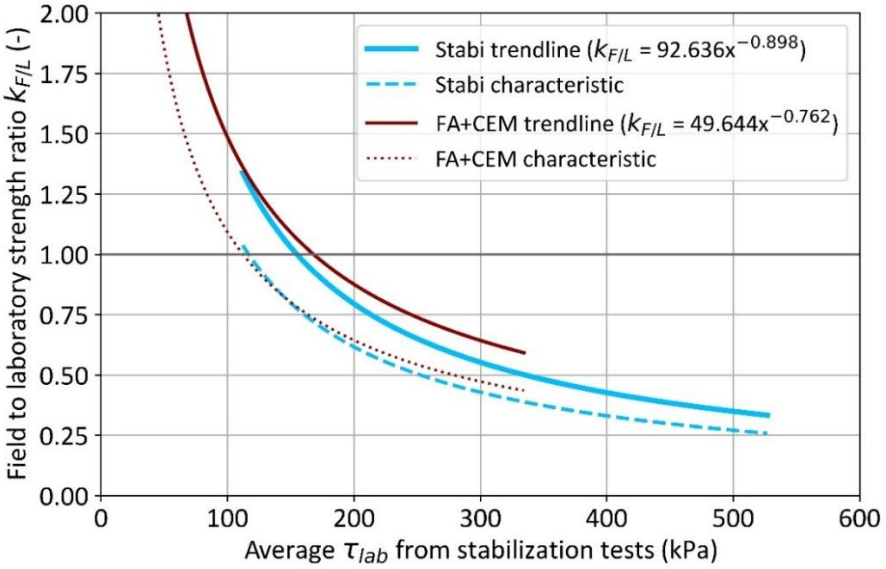


**Figure 26.** FA-containing binders (JAM+CEM II, KAI+CEM II, KAU+CEM II, Stabi65, and Stabi80). Trendline and the characteristic "cautious mean" curve for estimating the field to laboratory shear strength ratio from the average $\tau_{lab}$ for column-stabilized soil mixes.

## 4. Discussion

The design strength of the columns and the binder recipe can be determined most reliably on the basis of the results of QC soundings of the test columns or earlier production columns. When the QC sounding results of the columns implemented in the design area are not available, the design strength can be determined from the field to laboratory strength ratio and the results of the stabilization tests performed on the site's clay samples and potential binders.

It is widely accepted that in the laboratory, the mixture of binder and clay is more uniform than that of in situ columns. When mixing in situ columns using the dry method, a binder is blown into the mixing tool, which can cause loosening of the soil mix. For these reasons, higher strengths are usually achieved in the laboratory. On the other hand, the volume of the curing stabilization test specimen is a fraction of the volume of the curing column. For example, the cross-sectional area of a column with a diameter (D) of 700 mm is almost 200 times that of the D = 50-mm stabilization test specimen, and thus the volume of the stabilization test sample is only 0.05% of the volume of a 1-m-long D = 700 mm column. Hence, the in situ binder reaction is caused by a significantly larger amount of binder and soil mix, and the hardening temperature can be significantly higher, resulting in faster hardening of the in situ columns than for laboratory test specimens. The difference in the rate of curing of columns and laboratory specimens is the greatest at the beginning of curing, but the difference evens out quickly, which can be observed when examining, for example, the strengths of test columns and stabilization tests at curing ages of 7, 28, 50 and 90 d [19]. From 28 to 91 d, the field to laboratory shear strength ratio seems to decrease compared with the ratio at 7 days. In this article, all examinations are based on the shear strengths of test columns hardened for 28–90 d and stabilization tests, meaning that the effect of the initial curing rate has been minimized.

The COV and $\hat{s}_x$/avg values of the stabilization test results, which have been utilized in the result pairs ($k_{L/F}$), have been determined. The approximation method used to estimate the standard deviation $\hat{s}_x$ (Equation 5) has been formulated for a normal distribution, while the soil mix's shear strength is often assumed to follow a log-normal distribution. However, the estimated COV values for the variability of $\tau_{lab}$ are mostly in the range of 0.1–0.2 which indicates that the log-normal distribution closely resembles the normal distribution. Hence, the possible error arising from differing underlying probability distributions is estimated to be small. For the calcareous and gypsum-containing binders, the $COV_{av}$ and $\hat{s}_x$/avg values (28 + 91 d) are 0.07–0.10; for BFS-containing binders, they are 0.03–0.04; and for FA-containing binders, they are 0.03–0.07. According to the results, COV is clearly higher for calcareous and gypsum-containing binder types than for BFS- and FA-containing binder types. The COV values of the UCS results of the very extensive stabilization test series presented by Aalto [73] are at the same level: The lowest $COV_{av}$ (0.04) has been determined for the CEM II-stabilized soil mix while the highest $COV_{av}$ (0.07) has been determined for the lime cement-stabilized soil mix, and the $COV_{av}$ (0.05) in between has been determined for the GTC-stabilized soil mix.

The COV values thus determined were utilized in the statistical examinations. According to the statistical analyses, laboratory strength $k_{L/F}$ graphs that consider the underlying uncertainties have been determined using two approaches: Cautious trendlines based on the determined transformation uncertainty ($\delta$) and simulation-based validation. Simulation-based validation of the defined characteristic trendlines was performed using the average COV values based on stabilization test and QC sounding results. The characteristic trendline was found to be mostly in good agreement with the 31% percentiles calculated using the generated $k_{F/L}$ values. For all the studied binders, the 31% percentiles calculated from simulated values corresponded well with the characteristic "cautious" curve. In the newly derived graphs, the $k_{F/L}$ coefficient reduced with an increasing $\tau_{lab}$ and it is equal to1.0 when the shear strength determined by the stabilization tests is $\tau_{lab} \approx 100$ kPa with the binders KC, GTC, FA+CEM, and Stabi; $\tau_{lab} \approx 170$ kPa with the binders GREEN and POZ; and $\tau_{lab} \approx 220$ kPa with the binder CEM III. In the trendlines directly determined from the result pairs, before the statistical examinations, the $k_{F/L}$ ratio was 1.0 when the laboratory shear strength was 150–300 kPa. It is noteworthy that even though the 31% percentile was chosen as the definition of the characteristic cautious trendline in this study, the determined transformation uncertainties $\delta$ can be utilized to derive other percentiles too (e.g., 5%).

In connection with this work, the need for revision of the guidelines regarding the execution of QC soundings and analyzing the results has been recognized. The FTIA has planned revision work to take place in a few years. The need to supplement the QC guidelines has also been identified in other Nordic countries [79].

## 5. Conclusions

Extensive experimental field and laboratory strength data were collected and analyzed to study the variation in strength (COV) and the field to laboratory strength ratio of columns stabilized with lime cement and low-carbon binders. With low-carbon binders, the emissions related to deep mixing can typically be reduced by 60–70%. The binders investigated in this study can be divided into four groups according to their raw material compositions and performance: Calcareous, gypsum-containing, BFS-containing, and FA-containing.

The effect of the shear strength $\tau_{lab}$ achieved in the stabilization tests on the COV value has been examined for different binder types. The stabilization test results studied are from six test sites with column-stabilized soft clay or organic clay. According to the results, COV is clearly higher for calcareous and gypsum-containing binder types than for BFS- and FA-containing binder types ($COV_{av}$ 0.07–0.10 versus 0.03–0.07). The study considered curing times of 28 d and 90 d. The COV values for $\tau_{lab}$ are found to be of the same magnitude as the results presented earlier in the literature (see Figure 5). On the basis of the results, it cannot be said that the curing time of 28 d or 90 d influences the COV value.

The stabilization results show that the greatest shear strengths have been achieved with BFS-containing binders (CEM III/A and CEM III/B). Meanwhile, the lowest strengths have been achieved with FA+CEM II 7:3 mixtures, where the biomass incineration ash is directly from the silo and the dry ash is mixed with cement at the test site. The strengths of clay stabilized with calcareous and gypsum-containing binders were between the strengths achieved with the two binder types mentioned above.

Field to laboratory strength ratio nomograms have been formed from result pairs (274 pcs), where the field shear strength is based on the QC sounding results (660 diagrams) of the test columns and the laboratory shear strength $\tau_{lab}$ is based on the stabilization test results. The stabilization tests (1130 UCS tests) have been carried out with clay samples taken from the clay layers on which the test columns have been implemented. The same binder recipes and curing times have been used in the stabilization tests as in the test columns. The result pairs were compiled into figures with average $\tau_{lab}$ on the horizontal axis and field to laboratory strength ratio ($k_{F/L}$) on the vertical axis. Trendlines have been defined for the result pairs representing different binders, based on which, similar behavior was observed for all binder types: As the laboratory strength increases, the field to laboratory strength ratio decreases. As these field to laboratory strength ratio nomograms are affected by various sources of uncertainty, the characteristic "cautious mean" curves were derived in addition to trendlines fitted to the data. The transformation uncertainty (COV) related to predicting $k_{F/L}$ from the average $\tau_{lab}$ was found to be in the range of $\delta$ = 0.4–0.5.

The methods for determining the shear strength of soil mixes were the same as those used in Finland for the QC soundings of stabilized columns in deep mixing contracts and for stabilization tests in the design phase. The nomograms formed in this work will be utilized in the FTIA's next revision of the *Deep Stabilization Guidelines*, which is planned to be executed in 2026–2027. Prior to that, new test stabilizations and production-based stabilizations with low-carbon binders have been and will be implemented. Those results can be compared with the derived nomograms, and their compatibility can be validated. The 2001 nomogram in the FTIA guidelines does not consider, for example, the positive effect of loading during curing [13,55], which should also be included in the guidelines.

This article analyzed the macroscopic effects of various low-carbon binders. It is recommended that future studies incorporate relevant microstructural investigations (e.g., X-ray diffraction, Fourier transform infrared, scanning electron microscopy–energy-dispersive X-ray spectroscopy) to acquire more information on the chemistry of the soil and binder and their effects on curing at the test sites.

## Author contributions

Forsman wrote the article mainly. Löfman performed the statistical analysis for the field to

laboratory strength data. Ikävalko collected the QC sounding and stabilization test data and performed part of the laboratory tests. Korkiala-Tanttu commented on the article.

## Use of AI tools declaration

The authors declare they have not used artificial intelligence (AI) tools in the creation of this article.

## Acknowledgments

The authors would like to acknowledge the City of Helsinki, Vantaa, Porvoo, Tampere, and Lounais-Suomen Jätehuolto Oy (LSJH) for the test stabilizations. The authors thank Nordkalk Oy, Finnsementti Oy, UPM Kymmene Oy, and Pohjolan Voima Oy for the stabilization tests. The authors also acknowledge the Finnish Transport Infrastructure Agency, the Ramboll Foundation, and Aalto University for support for writing this article.

## Conflict of Interest

All authors declare no conflicts of interest in this paper.

## References

1. Institute of Environmental Management and Assessment, Pathways to Net Zero, Using the IEMA GHG Management Hierarchy, 2020. Available from: https://www.iema.net/media/bn3lgz1c/iema_ghg_hierarchy_nov_2020.pdf.
2. European Federation of Foundation Contractors (EFFC) and Deep Foundation Institute (DFI), EFFC/DFI Sustainability Guides for Foundation Contractors, Guide No. 1, Carbon Reduction, 2024. Available from: https://www.effc.org/content/uploads/2025/01/EFFC-DFI-Carbon_Reduction_Guide_2024_FINAL-1.pdf.
3. Perttu O, Vicente S, Löfman M, et al. (2024) Carbon management in geotechnical engineering solutions, *Geotechnical Engineering Challenges to Meet Current and Emerging Needs of Society*, CRC Press.
4. Freilich B, Martin K, Boehm D (2024) Sustainability in Practice: A Brief History of Innovation in Deep Soil Mixing. *Jap Geotech Soc Spec Publ* 11: 17–26. https://doi.org/10.3208/jgssp.vol11.KL-2
5. Kalpala T, Talja J (2025) Betolar Plc: Building the Future from Waste—High-Performing Green Cement Revolutionizes the Industry. Available from: https://www.sttinfo.fi/tiedote/71255723/betolar-plc-building-the-future-from-waste-high-performing-green-cement-revolutionizes-the-industry?publisherId=69820988&lang=fi.
6. Dejenie B, Raghuram A, Korkiala-Tanttu L, et al. (2024) Carbon Sequestration Capacity of Stabilized Soft Clays with Recycled Binders. *Geotech Test J* 47: 5–21. https://doi.org/10.1520/GTJ20220221

7. Hanafi M, Bordoloi S, Rinta-Hiiro V, et al. (2024) Feasibility of biochar for low-emission soft clay stabilization using $CO_2$ curing. *Transp Geotech* 49: 101370. https://doi.org/10.1016/j.trgeo.2024.101370
8. Hov S, Paniagua P, Sætre C, et al. (2023) Stabilisation of soft clay, quick clay and peat by industrial by-products and biochars. *Appl Sci* 13: 9048. https://doi.org/10.3390/app13169048
9. Viljanen M (2025) Concrete as a carbon sink—Carbonaide expands into international markets. Available from: https://teknologiateollisuus.fi/en/concrete-as-a-carbon-sink-carbonaide-expands-into-international-markets/.
10. Löfman M, Forsman J, Rintamo S, et al. (2023) Vähähiilinen esirakentaminen, opas, UUMA4-ohjelma, 129. In Finnish. Available from: https://uusiomaarakentaminen.fi/aineisto/vahahiilinen-esirakentaminen-opas/.
11. Frank R, Bauduin C, Driscoll R, et al. (2004) Designers's guide to EN1997-1: Eurocode 7: Geotechnical design—General rules. Telford. Available from: https://www.researchgate.net/publication/281048689_Designer's_guide_to_EN_1997-1_Eurocode_7_Geotechnical_design_-_General_rules.
12. Forsman J, Korkiala-Tanttu L, Koivisto K, et al. (2018) Syvästabiloinnin suunnittelu, Liikenneviraston ohjeita 17/2018. Helsinki, Finland: Finnish Transport Infrastructure Agency. In Finnish. Available from: http://web.archive.org/web/20230814092449/https://www.doria.fi/handle/10024/159212.
13. Kitazume M, Terashi M (2013) *The Deep Mixing Method*, London: CRC Press, 434.
14. EuroSoilStab, Design Guide Soft Soil Stabilisation. CT97-0351, Project No.: BE 96-3177. 2002. Available from: https://civilnode.com/download-book/10200730841441/design-guide-soft-soil-stabilisation-eurosoilstab-development-of-design-and-construction-methods-to-stabilise-soft-organic.
15. Ellen M, Bruce R, Berg J, et al. (2013) Federal Highway Administration Design Manual: Deep Mixing for Embankment and Foundation Support (no. FHWA-HRt-13-046). FWHA, United States. Federal Highway Administration. Offices of Research & Development. 248.
16. Horpibulsk S, Rachan R, Suddeepong A, et al. (2011) Strength development in cement admixed Bangkok clay: Laboratory and field investigations. *Soils Found* 51: 239–251. https://doi.org/10.3208/sandf.51.239
17. Madhyannapu R, Puppala A, Nazarian S, et al. (2010) Quality assessment and quality control of deep soil mixing construction for stabilizing expansive subsoils. *J Geotech Geoenviron Eng* 136: 119–128. https://doi.org/10.1061/(ASCE)GT.1943-5606.0000188
18. Timoney M (2015) *Strength verification methods for stabilised soil-cement columns: a laboratory investigation of PORT and PIRT*. The College of Engineering and Informatics, National University of Ireland, Galway, 521.
19. Andersson M, Vesterberg B (2016) Djupstabilisering av sulfidjord i två vägprojekt. Statens geotekniska institute SGI Publikation 32, Linköping. 84. Available from: https://bibliotek.vti.se/bib/284619.
20. Paniagua P, Hov S, Amiri A, et al. (2024) Recent Norwegian research on stabilisation of soft clays with the Dry Deep Mixing method. *Jap Geotech Soc Spec Publ* 11: 135–140. https://doi.org/10.3208/jgssp.vol11.DS-1-08

21. Savila I-M, Korkiala-Tanttu L, Forsman J, et al. (2025) Mechanical properties of stabilized soil: study on recovered field samples from deep stabilization sites. *Transp Geotech* 51. https://doi.org/10.1016/j.trgeo.2025.101540
22. Aalto A (1998) Syvästabilointi. A preliminary survey of Deep Mixing project, Helsinki University of Technology, 166. In Finnish.
23. Larsson S (2003) *Mixing Processes for Ground Improvement*. Doctoral thesis. Stockholm KTH, 218.
24. Larsson S (2021) The Nordic dry deep mixing method: best practices and lessons learned. *Deep Mixing-An Online Conference*. DFI Deep Foundation Institute.
25. Finnish National Road Administration, FinRA, Syvästabiloinnin mitoitusohje. Report 18/1997. TIEL 32000465, 25. 1997. Available from: https://doria.fi/bitstream/handle/10024/138791/3997tie.pdf?sequence=1&isAllowed=y.
26. Finnish National Road Administration, FinRA, Syvästabiloinnin suunnittelu, Tiehallinto. 2100008-v-04, 47. Deep stabilization design guide. 2001. In Finnish. Available from: https://www.tieh.fi/thohje/pdf/2100008_01.pdf.
27. Larsson S (2005) State of Practice Report—Execution, monitoring and quality control. *Deep Mixing* 5: 732–786.
28. Rakennustietosäätiö (2018) General specification for infrastructural construction works in Finland (InfraRYL, in Finnish), part 1 Earth, foundation and rock engineering, 424 and part 2 Pavement and surface structures, 413. Available from: https://www.rakennustietokauppa.fi/en/.
29. Löfman M, Forsman J, Järvinen K (2024) Kestävää aluerakentamista vähähiilisillä pohjanvahvistusmenetelmillä. In Finnish. Available from: https://www.ymparistojaterveys.fi/lehti/ymparisto-ja-terveys-lehti-7-2024/.
30. Löfman M, Vicente S, Perttu O, et al. (2024) Reducing the emissions from ground improvement by halve for the new part of Helsinki city—Case Malminkenttä. *Jap Geotech Soc Spec Publ* 11: 278–282. https://doi.org/10.3208/jgssp.vol11.DS-3-12
31. Wu J, Liu L, Deng Y, et al. (2022) Use of recycled gypsum in the cement-based stabilization of very soft clays and its micro-mechanism. *J Rock Mech Geotech Eng* 14: 909–921. https://doi.org/10.1016/j.jrmge.2021.10.002
32. Kujala K (1982) Kipsin käyttö syvästabiloinnissa. Licentiate thesis, Oulu University. In Finnish.
33. Kupryianchyk D, Song X (2021) *Stabilisering med alternativa bindemedel, Sammanställning av geotekniska egenskaper, klimatpåverkan och kostnad*, Statens Geotekniska Institute.
34. Arulrajah A, Yaghoubi M, Disfani M, et al. (2018) Evaluation of Fly Ash- and Slag-Based Geopolymers for the Improvement of a Soft Marine Clay by Deep Soil Mixing. *Soils Found* 58: 1358–1370. https://doi.org/10.1016/j.sandf.2018.07.005
35. Hoikkala S, Lahtinen P, Leppänen M (1996) Mass Stabilization of Peat in Road Construction. *Nordic Geotechnical Conference*, Reykjavik, Iceland: Icelandic Geotechnical Society. 391–395.
36. Kukko H (2000) Stabilization of clay with inorganic by-products. *J Mater Civ Eng* 12: 307–309. https://doi.org/10.1061/(ASCE)0899-1561(2000)12:4(307)
37. Lopez Ramírez A, Korkiala-Tanttu L (2023) Stabilisation of Malmi soft clay with traditional and low-$CO_2$ binders. *Transp Geotech* 38: 100920. https://doi.org/10.1016/j.trgeo.2022.100920
38. Janz M, Johansson SE (2002) The Function of Different Binding Agents in Deep Stabilization, Report 9. Linköping, Sweden: Swedish Deep Stabilization Research Centre.

39. Lahtinen P, Jyrävä H, Kuusipuro K (2000) Deep Stabilisation of Organic Soft Soils. *The International Conference on Ground Improvement Geosystems*, Helsinki, Finland: The Finnish Geotechnical Society, 89–98.
40. Ye G, Shu H, Zhang Z, et al. (2021) Solidification and Field Assessment of Soft Soil Stabilized by a Waste-Based Binder Using Deep Mixing Method. *Bull Eng Geol Environ* 80: 5061–5074. https://doi.org/10.1007/s10064-021-02193-7
41. Phoon KK, Kulhawy F (1999) Characterization of geotechnical variability. *Can Geotech J* 36: 612–624. https://doi.org/10.1139/t99-038
42. Forsman J, Löfman M, Ikävalko J, et al. (2025) Low-carbon binders in six test deep mixing cases —variation of in-situ strength. *Transp Geotech* 53. https://doi.org/10.1016/j.trgeo.2025.101597
43. Soveri U (1956) The mineralogical composition of argillaceous sediments of Finland: Ann. *Acad Sci Fennicae Ser A*, 32.
44. Keskinen R, Hillier S, Liski E, et al. (2022) Mineral composition and its relations to readily available element concentrations in cultivated soils of Finland. *Acta Agric Scand Sect B* 72: 751–760. https://doi.org/10.1080/09064710.2022.2075790
45. Löfman M (2022) *Uncertainty quantification for compressibility and settlement response of clays*, Aalto University.
46. Saresma M, Löfman M, Kosonen E, et al. (2023) Statistical approach to identify variables predicting sulphide clay occurrence in southern Finland. *Bull Eng Geol Environ* 82: 257. https://doi.org/10.1007/s10064-023-03258-5
47. Ilonen E, Itkonen J, Kajankari-Shelvey P, et al. (2024) Pilaristabiloinnin ympäristövaikutukset, Malminkentän pilaristabiloinnit 2022. Report. In Finnish.
48. Korhonen KH, Gardemeister R, Tammirinne M (1974) Geotekninen Maaluokitus. Espoo, Finland: Valtion Teknillinen Tutkimuskeskus VTT. In Finnish. Available from: https://cris.vtt.fi/en/publications/geotekninen-maaluokitus/.
49. SFS-EN ISO 17892-1:fi, 2015-01-19, Geotechnical investigation and testing, 2015. Available from: https://sales.sfs.fi/fi/index/tuotteet/SFS/CENISO/ID2/1/1122819.html.stx.
50. SFS-EN 17685-1:2023, Earthworks. Chemical tests. Part 1: Determination of loss on ignition. 2023. Available from: https://sales.sfs.fi/fi/index/tuotteet/SFS/CEN/ID2/1/1232705.html.stx.
51. ISO 10390, Soil, treated biowaste and sludge—Determination of pH. 2021. Polish Committee for Standardizations: Warsaw, Poland, 2022.
52. Deutsches Institut für Normung, Water quality. Determination of selected elements by inductively coupled plasma optical emission spectrometry (ICP-OES) (ISO 11885:2007), Beuth Verlag GmbH, 2009.
53. SFS-EN ISO, Geotechnical investigation and testing. Field testing. Part 9: Field vane test (FVT and FVT-F) (ISO 22476 9:2020), 2020. Available from: https://www.iso.org/standard/73643.html.
54. DIN EN, 15643: Sustainability of construction works: Framework for assessment of buildings and civil engineering works. Helsinki, SFS ry, 39. 2021.
55. Åhnberg H (2006) *Strength of stabilised soils—A laboratory study on clays and organic soils stabilised with different types of binder*. Doctoral Thesis, Lund University. 202.

56. AVI. Aluehallintovirasto (2024) Päätös nro 79/2024, LSSAVI/12005/2023. Asia: Jämsänkosken voimalaitoksen ympäristöluvan muuttaminen, Jämsä. In Finnish. Available from: https://avi.fi/en/registry.
57. Nguyen T (2021) *Uusiosideaineet pilaristabiloinnissa, Kuninkaantammen koestabilointi*. Master thesis. Aalto University, 154. In Finnish.
58. Oy KT (2022) Kaukaan Voima Oy:n lentotuhkan hyötykäyttö- ja kaatopaikkakelpoisuuden tutkimus 1/2022. Finnish: Kaukaan Voima Oy's study on the utilisation and landfill suitability of fly ash 1/2022, 2022, 4. In Finnish.
59. Silmu R (2025) Personal communication (e-mail) to. J Forsman 2025; 21:5.
60. Ecolan (2019) Suoritustasoilmoitus Nro 1. Rev. 19. (*Declaration of performance*). In Finnish. Available from: https://www.ecointellect.fi/en/contact-us/.
61. Forsman J, Ikävalko J, Löfman M, et al. (2024) Stabilization tests for deep mixing—round-robin tests in eight Finnish laboratories. *Geotech Test J* 47: 948–965. https://doi.org/10.1520/GTJ20230377
62. Leinonen T, Forsman J (2022) Topinpuisto, Turku. Yhteenveto koestabiloinnin ympäristö-tutkimuksista. Loppuraportti 18.11.2022. In Finnish. Available from: https://uusiomaarakentaminen.fi/wp-content/uploads/sites/5/2023/11/Topinpuisto-Turku-Yhteenveto-koestabiloinnin-ymparistotutkimuksista.pdf.
63. Nordkalk, Environmental product declaration. Nordkalk Terra KC products, Nordkalk Terra GTC, Nordkalk Terra GREEN and Nordkalk Terra POZ products, 2025. Available from: https://nordkalk.fi/nordkalkin-terra-tuotteille-epd-sertifikaatit-askel-kohti-vastuullisempaa-rakentamista/.
64. Kuusipuro K (2025) e-mail to J. Forsman 27.3.2025.
65. Ikävalko J (2023) *Pilaristabiloinnin kenttä- ja laboratoriolujuuksien suhde koestabilointikohteissa*. Master thesis. Aalto University, 223. In Finnish. Available from: https://aaltodoc.aalto.fi/items/3f6f0026-a308-4a87-ad39-7d0184db5bbd
66. Koivulahti M, Jyrävä H, Niemelin T, et al. (2019) Deep soil mixing—Finnish guideline for stabilisation tests, *European Conference on Soil Mechanics and Geotechnical Engineering*, Icelandic Geotechnical Society.
67. Halkola H (1999) Keynote lecture: Quality control for dry mix methods, *Dry Mix Methods of Deep Soil Stabilization*, Routledge.
68. Forsman J, Melander M, Winqvist F (2017) Mass stabilization quality control methods, *Proceedings of the 19th International Conference on Soil Mechanics and Geotechnical Engineering*, Seoul.
69. Kitazume M, Terashi M, Tokunaga S (2021) Importance of water/cement ratio concept in quality control and assurance of deep mixed soil. *Deep Mixing' 2020: Best Practice and Legacy June 2021 Online Workshop*. Available from: https://www.issmge.org/events/dfi-deep-mixing-conference-2021-an-online-conference.
70. Löfman M, Korkiala-Tanttu L (2021) Inherent variability of geotechnical properties for Finnish clay soils, *18th International Probabilistic Workshop*, IPW 2021. Lecture Notes in Civil Engineering, Springer, Cham. https://doi.org/10.1007/978-3-030-73616-3_32

71. Knuuti M, Löfman M (2022) Epävarmuudet ja luotettavuus geoteknisessä mitoituksessa, Luotettavuus-workshop 2022. Väyläviraston julkaisuja. In Finnish.
72. Åhnberg H, Holm G (2009) Influence of Laboratory Procedures on Properties of Stabilized Soil Specimens. *International Symposium on Deep Mixing and Admixture Stabilization,* Okinawa, Japan: Port and Airport.
73. Aalto A (2006) Indeksikokeet, Tietoverkottunut, 3D-mallinnukseen ja -mittauksiin perustuva pohjavahvistusautomaatio. Helsinki University of Technology, 135. In Finnish.
74. Kitazume M (2024) Deep mixing technology—diversity and future development. *Jap Geotech Soc Spec Publ* 11: 1–16. https://doi.org/10.3208/jgssp.vol11.KL-1
75. Piispanen P (2017) *Massastabiloinnin pitkäaikaistoimivuus*. Master thesis. Aalto University, 115. In Finnish.
76. Bergman N, Al-Naqshabandy M, Larsson S (2013) Variability of strength and deformation properties in lime-cement columns evaluated from CPT and KPS measurements. *Georisk* 7: 21–36. https://doi.org/10.1080/17499518.2013.763571
77. Al-Naqshabandy M, Bergman N, Larsson S (2012) Strength variability in lime-cement columns based on cone penetration test data. *Proc Inst Civ Eng Ground Improv* 165: 15–30. https://doi.org/10.1680/grim.2012.165.1.15
78. Wong D, Sadasivan V, Isaksson J, et al. (2024) Trans-scale spatial variability of lime-cement mixed columns. *Constr Build Mater* 417: 135394 https://doi.org/10.1016/j.conbuildmat.2024.135394
79. Hov S, Moe E, Haraldsen G, et al. (2025) Laboratory scale column penetration tests for deep mixing purposes. *Can Geotech J* 62: 1–14. https://doi.org/10.1139/cgj-2024-0811
80. Guimond-Barrett A (2013) *Influence of mixing and curing conditions on the characteristics and durability of soils stabilised by deep mixing*. Doctoral thesis. Université du Havre, 261.
81. Burke G, Sehn A (2005) An Analysis of Single Axis Wet Mix Performance. *Deep Mixing '05: International conference on deep mixing best practice and recent advances*, Stockholm.
82. Navin M, Filz G (2005) Statistical Analysis of Strength Data from Ground Improved with DMM Columns. *Deep Mixing* 5: 145–154.
83. Baecher GB, Christian JT (2023) *Reliability and Statistics in Geotechnical Engineering*, John Wiley & Sons, Chichester, UK.
84. Burington R, May D (1970) *Handbook of Probability and Statistics with Tables*, 2nd Ed. New York: McGraw Hill.
85. Snedecor G, Cochran W (1989) *Statistical Methods*, 8th Edition, Iowa State University Press, Ames.
86. Ching J, Phoon KK (2014) Transformations and correlations among some clay parameters—The global database. *Can Geotech J* 51: 663–685. https://doi.org/10.1139/cgj-2013-0262
87. Schneider H (1997) Definition and characterization of soil properties. *Proceedings of the 14th International Conference on Soil Mechanics and Geotechnical Engineering*, Hamburg. Balkema, Rotterdam, 2271–2274.
88. Löfman M, Korkiala-Tanttu L (2022) Transformation models for the compressibility properties of Finnish clays using a multivariate database. *Georisk* 16: 330–346. https://doi.org/10.1080/17499518.2020.1864410

89. Phoon K-K, Tang C (2019) Characterization of geotechnical model uncertainty. *Georisk* 13: 101–130. https://doi.org/10.1080/17499518.2019.1585545
90. Ching J, Noorzad A (2021) Statistics for transformation uncertainties. State-of-the-art review of inherent variability and uncertainty in geotechnical properties and models. Available from: https://issmge.org/files/reports/TC304-State-of-the-art-review-of-inherent-variability-and-uncertainty-in-geotechnical-properties-and-models.pdf.


AIMS Press